Tellus (2008), 60B, 583–603
Printed in Singapore. All rights reserved

TELLUS

Simulating effects of land use changes on carbon fluxes: past contributions to atmospheric CO_2 increases and future commitments due to losses of terrestrial sink capacity

By K. M. STRASSMANN[1]*, F. JOOS[1] and G. FISCHER[2], [1]*Climate and Environmental Physics, Physics Institute, University of Bern, Bern, Switzerland;* [2]*International Institute for Applied Systems Analysis, A-2361 Laxenburg, Austria*

(Manuscript received 31 June 2007; in final form 20 December 2007)

ABSTRACT

The impact of land use on the global carbon cycle and climate is assessed. The Bern carbon cycle-climate model was used with land use maps from HYDE3.0 for 1700 to 2000 A.D. and from post-SRES scenarios for this century. Cropland and pasture expansion each cause about half of the simulated net carbon emissions of 188 Gt C over the industrial period and 1.1 Gt C yr^{-1} in the 1990s, implying a residual terrestrial sink of 113 Gt C and of 1.8 Gt C yr^{-1}, respectively. Direct CO_2 emissions due to land conversion as simulated in book-keeping models dominate carbon fluxes due to land use in the past. They are, however, mitigated by 25% through the feedback of increased atmospheric CO_2 stimulating uptake. CO_2 stimulated sinks are largely lost when natural lands are converted. Past land use change has eliminated potential future carbon sinks equivalent to emissions of 80–150 Gt C over this century. They represent a commitment of past land use change, which accounts for 70% of the future land use flux in the scenarios considered. Pre-industrial land use emissions are estimated to 45 Gt C at most, implying a maximum change in Holocene atmospheric CO_2 of 3 ppm. This is not compatible with the hypothesis that early anthropogenic CO_2 emissions prevented a new glacial period.

1. Introduction

Past and current land use and land use changes (LULUC) contribute to the ongoing anthropogenic climate change (Forster et al., 2007). LULUC activities continue to cause large emissions of carbon dioxide (Houghton et al., 1983; McGuire et al., 2001; Achard et al., 2002; DeFries et al., 2002; Houghton, 2003) and other greenhouse gases (Strengers et al., 2004) to the atmosphere and alter surface properties such as albedo and water vapour exchange (Feddema et al., 2005; Sitch et al., 2005). Presently, about 40% of the world's vegetated land surface (excluding deserts, barren and ice-covered land) is used as cropland or pasture (Klein Goldewijk, 2001). While land use change has many socio-economic and climatic consequences, here, we are interested in the impact of LULUC on the global carbon cycle and atmospheric CO_2 and CO_2 related climatic changes over the industrial period and the future.

*Corresponding author.
e-mail: strassmann@climate.unibe.ch
DOI: 10.1111/j.1600-0889.2008.00340.x

Uncertainties in the quantitative understanding of the impact of LULUC on the global carbon cycle lead to uncertainties in projections of atmospheric CO_2 and climate, and consequently, affect the formulation of emission mitigation strategies. Carbon fluxes due to LULUC constitute the least well quantified flux in the global carbon budget (Pacala et al., 2001; Prentice et al., 2001; Goodale et al., 2002; Houghton et al., 2004; Denman et al., 2007).

Carbon emissions from LULUC have traditionally been estimated by a book-keeping method (Houghton et al., 1983) that takes into account temporal delays between carbon emissions and uptake after deforestation or abandonment of used land. This approach neglects any feedback between atmospheric CO_2, climate and carbon emissions from LULUC (Leemans et al., 2002). Changes in management practices such as fire suppression, thinning or grazing (Hurtt et al., 2002; Nabuurs et al., 2003; Field and Raupach, 2004; Vesala et al., 2005) are often neglected, too.

Carbon fluxes due to LULUC estimated with book-keeping methods have been used in coupled carbon cycle-climate models (Prentice et al., 2001; Meehl et al., 2007). LULUC fluxes were exogenously prescribed in analogy to fossil emissions. It has been postulated that land carbon storage is overestimated in

such simulations, since no correction is made for the increasing area under cultivation, where carbon turnover is faster and sink capacity reduced compared to area covered by forests (Gitz and Ciais, 2004). This limitation can be overcome by endogenous modelling of LULUC processes based on spatially explicit land use maps. Previous global studies taking this approach used terrestrial models either forced by prescribed climate fields and atmospheric CO_2 (McGuire et al., 2001) or run as a module in coupled carbon cycle-climate model (e.g., Leemans et al., 2002; Sitch et al., 2005; Brovkin et al., 2006). Except Leemans et al. (2002), these studies considered changes in cropland and neglected the impact of changes in pasture area.

These studies highlight the importance of accurate spatially explicit fields that describe the spatio-temporal evolution of the area under land use for assessing LULUC impacts. Such maps have recently become available for cropland (Ramankutty and Foley, 1999) and for cropland, pasture and built-up area (Klein Goldewijk, 2001, 2005; Klein Goldewijk and van Drecht, 2006) for the industrial period. Land use maps are also part of the output of some integrated assessment models used to develop mitigation and non-mitigation emission scenarios (Nakićenović and Swart, 2000; Strengers et al., 2004; Riahi et al., 2007) for the 21st century. In combination, these products provide the opportunity to study the evolution of land use, atmospheric CO_2 and climate over the industrial period and this century in a consistent way (Strengers et al., 2004).

Recently, a new set of emission scenarios have become available that incorporate the latest progress in scenario development (Riahi et al., 2007). In addition to these plausible scenarios, IPCC illustrates in its Fourth Assessment Report inertia in the climate system by analysing the commitment of past and 21st century emissions on future climate (Meehl et al., 2007). In these commitment scenarios either radiative forcing is kept at the value reached in year 2000 (or year 2100), or emissions are instantaneously reduced to zero in 2000 (or 2100). In none of these analyses, the inertia of LULUC processes has been addressed.

Here, we apply the Bern Carbon Cycle-Climate (BernCC) model (Joos et al., 2001; Gerber et al., 2003, 2004; Joos et al., 2004) that includes the Lund-Potsdam-Jena Dynamic Global Vegetation Model (LPJ-DGVM) (Sitch et al., 2003) complemented with a new module describing LULUC processes to address a range of LULUC related research questions. The most recent maps from the History Database of the Global Environment (Klein Goldewijk and van Drecht, 2006) and from the most recent post-SRES scenarios from the Institute of Applied System Analyses (Riahi et al., 2007) are used to force the BernCC model. The BernCC model is cost-efficient, allowing us to perform a complete set of sensitivity simulations used to disentangle qualitatively different processes contributing to the LULUC impact and to quantify their relative importance over time.

The goals of this study are: (i) to estimate carbon emissions from LULUC over the industrial period and the past decades in the BernCC model framework, thereby contributing to the ongoing assessment of the magnitudes und uncertainties of LULUC induced carbon fluxes; (ii) to make an appraisal of the potential impact of pre-industrial LULUC on atmospheric CO_2 and climate; (iii) to project atmospheric CO_2 and climate in three new scenarios for 21st century land use and emissions of CO_2 and other anthropogenic forcing agents; (iv) to quantify the different environmental feedbacks and interactions of LULUC with past and future atmospheric CO_2 employing a range of factorial model experiments and (v) to assess the impact of past LULUC on future atmosphere-land carbon fluxes, atmospheric CO_2, and climate. We invoke the concept of a land use commitment to characterize this impact.

2. Methods

Sections 2.1 and 2.2 describe the boundary conditions used to drive the simulations (Fig. 1). These include estimates of past LULUC and scenarios of LULUC and industrial emissions for this century. The data provided by other research groups were processed for use within BernCC as detailed below. Sections 2.3–2.5 explain key model features and simulation procedures. Section 2.6 describes an analytical framework for decomposing the impact of LULUC into qualitatively different processes.

2.1. Land use data

The HYDE database (version 3.0) from Klein Goldewijk and van Drecht (2006) describes the geographically explicit evolution of

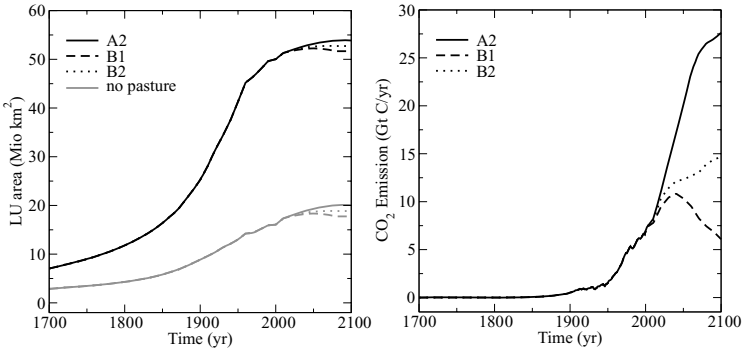

Fig. 1. Left-hand side: global land use area for past 300 yrs and scenarios A2, B1 and B2. Right-hand side: CO_2 emissions from fossil fuel use and cement production estimated for the industrial period (Marland et al., 2006) and projected for this century for the IIASA scenarios A2, B1 and B2.

croplands, of pastures and of urban (built-up) areas for the period from 1700 to 2000. The urban land class was not included in the previous HYDE2.0 database (Klein Goldewijk, 2001). The HYDE data have a resolution of 5 arcmin in space and of 10 yr in time. For the future, the Land Use Change (LUC) group at IIASA has developed maps of cropland and built-up area for a range of (updated, post-SRES) emissions scenarios based on the SRES storylines (Tubiello and Fischer, 2006). The land use distribution for year 2000 is derived from remote sensing satellite products from the National Oceanic and Atmospheric Administration Advanced Very High Resolution Radiometer (NOAA-AVHRR) and from the Global Land Cover Project (GLC2000) (Tubiello and Fischer, 2006). A map is supplied for each decade until 2100 based on global food demand and supply simulations with IIASA's linked agroecological zones (AEZ) model and world food system (BLS) model (Tubiello and Fischer, 2006). Data are given as cropland and built-up area fractions for each grid cell of $0.5^\circ \times 0.5^\circ$. The evolution of pasture is not specified by the IIASA data.

The data are aggregated onto the BernCC model grid of 3.75° longitude by 2.5° latitude. The area fractions occupied by pasture p, cropland c and built-up area b (identified with the urban class in HYDE3.0) are specified for each cell. Only the net land use changes on the grid cell level are modelled. Consequently, when new land is claimed while used land is abandoned within the same aggregated cell, the model 'sees' a net change smaller than the area experiencing land use change. In this way, about 15% of gross land use change is masked by the aggregation. The corresponding bias to carbon fluxes should be smaller, since losses from reclaimed land will be partly compensated by regrowth on abandoned land. The total land area in the coarse model grid is slightly smaller than that of the original map. Land use area was conserved in the aggregation to prevent a bias on the rates of land use change. Consequently, the percentage of the global land cover under land use is increased in the process (37% instead of 33% in 2000 A.D.).

The land use data from HYDE3.0 and IIASA are combined into a land use evolution that exhibits a seamless transition between the HYDE and IIASA data sets, as discontinuities would lead to spurious carbon fluxes. The land use distribution for year 2000 is well established from satellite data and ground truth and is kept unchanged in the combined land use data set. The IIASA scenarios, consistent with the year 2000 data are also used without further modification. The HYDE data for the past, which are more uncertain than the present land use map, are adjusted to blend in with the IIASA data at year 2000. Test simulations with the original HYDE3.0 data yield very similar results with respect to global carbon fluxes and climate as the simulations with the adjusted data. The specific adjustment procedure is as follows.

The cropland fraction c is calculated as

$$c(t) = \min\left[1,\, c_{\mathrm{IIASA}}(2000) \cdot \frac{c_{\mathrm{HYDE}}(t)}{c_{\mathrm{HYDE}}(2000)}\right] \quad \forall\, t < 2000. \quad (1)$$

Thus, the spatial pattern is taken from the IIASA map at 2000, and the history of each cell is scaled according to the HYDE data. The minimum condition is necessary because in some cells, cropland has a maximum in the past which may become greater than unity when scaled with the IIASA map of 2000. In cells where cropland exists in the IIASA map but not in the HYDE map, this approach is not applicable. Here, the latitudinally nearest cropland cell from HYDE was used for scaling.

A similar procedure was applied for cells with built-up areas in both data sets,

$$b(t) = \min\left[1 - c(t),\, b_{\mathrm{IIASA}}(2000) \cdot \frac{b_{\mathrm{HYDE}}(t)}{b_{\mathrm{HYDE}}(2000)}\right] \quad \forall\, t < 2000, \quad (2)$$

where b is restricted to the area not already occupied by c. Built-up areas are sparse and the scaling procedure applied to cropland could not be used for cells lacking built-up areas in HYDE. Instead, these cells were scaled using average HYDE built-up densities, calculated on a very coarse grid of 30×30 degrees to capture the basic differences in the timing of development.

The evolution of pasture was taken directly from the HYDE3.0 data, as the IIASA data do not contain information about pastures

$$p(t) = \min[1 - c(t) - b(t),\ \ p_{\mathrm{HYDE}}(t)\,] \quad \forall\, t \le 2000\,, \quad (3)$$

again with the condition that the combined area fractions $c + b + p$ do not exceed unity. For times later than 2000, the same formula is used with $p_{\mathrm{HYDE}} = p_{\mathrm{HYDE}}(2000)$. In other words, pastures remain in continued use unless space is required for cropland or built-up area. We resort to this not very plausible assumption due to the lack of future scenarios of pasture development. This is clearly a limitation that should be addressed in future studies. The projected net change in the total area under land use (crop, pasture, built-up) is about 15% smaller than the net change in cropland area. Often new cropland is assumed to be established on pasture land to meet the requirement that total land use area does not exceed the grid cell area.

Figure 1 shows the development of the global cropland and built-up area and of pasture for the industrial period and for the IIASA scenarios A2, B1 and B2.

2.2. *Emission and land cover scenarios*

Emission scenarios for the SRES storylines A2, B1 and B2 were developed at IIASA, running the MESSAGE model and the DIMA model in a coupled mode (Rokityanskiy et al., 2006; Riahi et al., 2007). The DIMA and MESSAGE models simulate forestry activities and related carbon fluxes based on demand and prices for wood for energy and other uses. For each storyline, a baseline case (no climate specific policy measures) and a mitigation case (includes climate policy) has been simulated. Forestry for wood production is expected to have a small net effect on the carbon budget in the baseline scenarios, as harvest tends to be compensated by regrowth (Houghton, 2003). In the mitigation

cases, important carbon uptake fluxes are simulated by DIMA as a result of forest management for carbon sequestration and bioenergy production. The BernCC model does not include formulations for forest management nor bioenergy production, and cannot therefore reasonably represent the mitigation scenarios. Accordingly, we use the baseline scenarios, where DIMA and BernCC are broadly comparable. Global land use area for each scenario including the historical period is given in Fig. 1.

MESSAGE calculates decadal industrial emissions of the major radiative forcing agents or precursors based on quantifications of the SRES storylines in terms of economic growth, population growth and technological change (Messner and Schrattenholzer, 2000). Here, the industrial emissions of CO_2 (Fig. 1), CH_4, N_2O, NO_x, CO, VOC, SO_2, CF_4, C_2F_6, SF_6, HFC125, HFC134a, HFC143a, HFC227e and HFC245c from MESSAGE and the spatio-temporal evolution of land cover are prescribed in the BernCC model to calculate atmospheric concentrations, radiative forcing, and climate change for the post-SRES baseline scenarios A2, B1 and B2. The industrial CO_2 emissions from these scenarios are shown in Fig. 1, together with historical emissions from Marland et al. (2006). These post-SRES scenarios are similar to the corresponding IPCC SRES scenarios and span a range of projections comparable to the set of illustrative SRES scenarios (Prather et al., 2001).

2.3. Model

The BernCC model is a cost-efficient carbon cycle-climate model. It includes chemistry, radiative forcing, climate and carbon cycle modules to simulate the evolution of CO_2 and other radiative agents and climate. A detailed model description can be found elsewhere (Joos et al., 2001). The BernCC model has been applied in a range of studies to investigate the coupling between the carbon cycle and climate change both in the past and in the future and over decadal to millennial time scales (Joos et al., 2001; Gerber et al., 2003, 2004; Edmonds et al., 2004; Joos et al., 2004; Köhler et al., 2005). The BernCC model and its variants have also been used to project atmospheric CO_2 in the Second (Schimel et al., 1996), Third (Prentice et al., 2001) and Fourth (Meehl et al., 2007) Assessment Report of IPCC. Here, the BernCC model has been extended by implementing formulations for LULUC as described in Section 2.4.

The model's climate component is an impulse response-empirical orthogonal function (IRF-EOF) substitute of the ECHAM3/LSG (Cubasch et al., 1997) driven by radiative forcing. We do not consider the range of different and newer AOGCM behaviours as summarized e.g. in Meehl et al. (2007). Some models exhibit additional strong climate-carbon cycle interactions (e.g. drying of the Amazon region). We regard this limitation as not critical for the focus of this study, the role of LULUC for the carbon cycle, which does not show a strong dependence on climate change (see Section 3.6). The equilibrium climate sensitivity is set to 2.5° C for a doubling of atmospheric CO_2. Atmospheric loading and radiative forcing are calculated from emissions using parametrized expressions derived from complex models (Prather et al., 2001).

The carbon cycle module simulates the redistribution of CO_2 within the Earth system. It consists of a well-mixed atmosphere, the High-Latitude Exchange/Interior Diffusion-Advection (HILDA) ocean model (Joos et al., 1996; Siegenthaler and Joos, 1992), and the Lund-Potsdam-Jena Dynamic Global Vegetation Model (LPJ DGVM) (Sitch et al., 2003).

The LPJ DGVM is widely used by the community and has been applied in a range of studies investigating changes in the terrestrial system (e.g. McGuire et al., 2001; Sitch et al., 2003, 2005; Bondeau et al., 2007; Mikolajewicz et al., 2007). LPJ simulates changes in vegetation distribution, terrestrial pools and fluxes of carbon and its stable isotope (^{13}C), and the terrestrial water balance. In the BernCC model framework, LPJ is driven interactively by the simulated atmospheric CO_2 and spatial fields of temperature, precipitation and cloud cover.

The version used in BernCC simulates the distribution of nine natural plant functional types (PFTs) based on bioclimatic limits for plant growth and regeneration and plant specific parameters that govern plant competition for light and water. There are six carbon pools per PFT, representing leaves, sapwood, heartwood, fine roots, aboveground and belowground litter, and two soil carbon pools, which receive input from litter of all PFTs. Photosynthesis is modelled using a form of the Farquhar scheme (Farquhar et al., 1980) with leaf-level optimized nitrogen allocation (Haxeltine and Prentice, 1996) and an empirical convective boundary layer parametrization (Monteith, 1995) to couple the carbon and water cycles. Decomposition rates of soil and litter organic carbon depend on soil temperature (Lloyd and Taylor, 1994) and moisture (Foley, 1995). Fire fluxes are calculated from litter moisture content, a fuel load threshold, and PFT specific fire resistances. Soil texture classes are assigned to every grid cell (Zobler, 1986), and the soil hydrology is simulated using two soil water layers. The light routine has been revised as detailed in the appendix compared to the version described by Sitch et al. (2003) and used in earlier applications of the BernCC model. The spatial resolution of the LPJ-DGVM is set to $3.75° \times 2.5°$; this coarse resolution version yields practically identical results as a version with a resolution of $0.5° \times 0.5°$ (Mueller and Lucht, 2007).

2.4. Implementation of a land use module in LPJ-DGVM

Each grid cell of LPJ is split into fractions reserved for natural vegetation, agriculture including cropland and pasture, and built-up areas.

Fractions change over time according to the spatio-temporal evolution of land cover (Section 2.1). This fractional approach is advantageous, because it permits the continuous adjustment of the area under land use as opposed to the often used approach where a cell is either entirely under land use or entirely natural

vegetation. It also allows to differentiate between built-up area and other forms of land use.

Natural vegetation is simulated as in the original LPJ, the only difference being that it is restricted to the area fraction of each cell not reserved for land use. Consequently, the PFT distribution on the natural cell fraction is not prescribed externally, but dynamically simulated. While this approach is limited in the accuracy of past land cover representations, it offers the advantage that the effect of future vegetation changes in response to changing climate and CO_2 (e.g., biome shifts) is captured by the model.

It is often assumed that pastures are preferentially claimed from natural grasslands (e.g. Houghton, 1999). Preferential conversion of grasslands within a single cell cannot be reconciled conceptually with the approach of LPJ, which represents natural vegetation as a mixture of PFTs. This may lead to an overestimation of CO_2 emissions due to pasture expansion (cf. Section 4).

Cropland and pasture are represented by the natural grass PFTs (C3 or C4 depending on climatic conditions). Tree PFTs and fires are excluded from the agricultural cell fraction. Bondeau et al. (2007) have recently developed a suite of different PFTs representing different agricultural crops. Specific crop PFTs only slightly affect the net carbon balance, which is the focus of this study. Thus it is adequate to our purpose to use grass PFTs instead. On built-up area, plant growth is suppressed. The carbon and water cycles and plant growth on each cell fraction are independent. Interactions among cell fractions occur only when land is converted from one category to another.

Figure 2 illustrates the changes in carbon and soil water pools resulting from conversion of natural land to pasture or cropland. The content of the natural pools only changes in proportion to the area lost and the carbon and water densities within the natural areas remain unchanged. The fraction of carbon and water previously allocated on the converted natural land is transferred to the land use fraction and to product pools. The carbon and water densities on used land are adapted taking into account the expansion in area and the input from the converted natural land (arrow A). Carbon in leaves and roots from converted natural land is transferred as slash and dead organic carbon to the litter pools, whereby the combined mass of carbon in leaves, roots and litter compartments is conserved. In contrast to book-keeping models, the fate of litter and soil carbon input from land conversions is not prescribed explicitly (e.g. by response functions), but governed by LPJ's parametrizations of organic matter decay, which depend on soil moisture, air, and soil temperature.

Carbon in heartwood and sapwood is removed and 25% is directed to the atmosphere and 75% by equal parts to two product pools (arrow B). Carbon in the product pools decays exponentially with an e-folding time of 2 and 20 yr, respectively. This product routing scheme is the same as in the DIMA model. It neglects differences in harvesting practices and wood extraction among different regions (Houghton, 1999). However, the details of the product pools are not critical for our decadal-to-century scale analysis of LULUC and climate. The same procedure is applied for the conversion of natural land to built-up area.

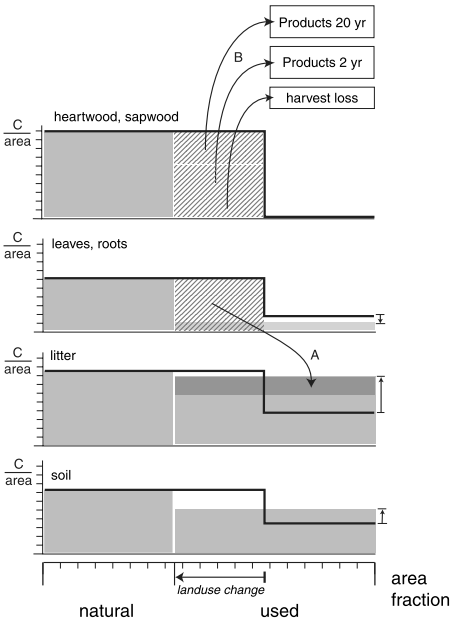

Fig. 2. Redistribution of carbon during the transformation of natural land to cropland and pasture. The horizontal axis indicates the split of a given cell into natural vegetation and agricultural land (built-up area is omitted for simplicity). The vertical axes indicate carbon density on natural or used land in different compartments. Thus, the carbon content per grid cell of each pool corresponds to the area of the individual boxes. The arrow on the horizontal axis indicates a reduction of natural and expansion of used land (conversion). The state before the conversion is shown by the bold lines. The state immediately after the conversion is shown by gray boxes. Carbon densities on used land change upon conversion as indicated by the vertical arrows on the right-hand side.

Abandonment of used land is modelled analogously, except that no wood products are generated. Abandoned land is merged with natural land, whereby in the case of forest growth, no distinction between primary and secondary forests is made.

As the focus of this study is on the terrestrial carbon balance, changes in albedo and the coupling of the terrestrial water cycle and climate are not modelled. The radiative forcing related to albedo changes in response to LULUC is small compared to the radiative forcing by greenhouse gases (Forster et al., 2007). The coupling of the terrestrial water cycle and the atmosphere can lead to significant changes in local to regional climate (Seneviratne et al., 2006) and caution must be used when interpreting regional changes in LPJ. However, fully coupled simulations with the state-of-art NCAR Community Climate System Model yield a relatively small impact of this coupling on simulated global climate change (Feddema et al., 2005).

Table 1. Simulated net biospheric uptake in Gt C. Shown are integrated fluxes over the historical period, and the 21st century for scenario A2 and A2 with land use area kept constant after 2000 A.D. ('A2 commitment'). Results are for simulations with natural vegetation ('no LU'), with prescribed pasture, cropland and built-up area ('LU'), and with prescribed cropland and built-up area ('no pasture'). Model settings are indicated in the first three columns. The simulations with simulated and prescribed CO_2 yield identical results when both CO_2 fertilization and climate change are shut off (bottom row). Dashes indicate settings for which no simulation was performed

Historical CO_2	Climate change	CO_2 fertil.	historical 1700–1999			A2 2000–2099			A2 commitment 2000–2099	
			No LU	LU . . . no pasture		No LU	LU . . . no pasture		LU . . . no pasture	
Simulated	✓	✓	73.3	−115.0	−10.4	264.9	53.5	153.2	114.6	208.8
Simulated	✓	×	−5.0	−254.9	−118.1	−275.4	−326.2	−318.2	−282.9	−275.1
Simulated	×	✓	75.0	−101.4	−2.8	468.1	302.0	370.2	–	–
Prescribed	✓	✓	126.7	−123.1	13.4	248.7	58.5	142.6	119.9	202.9
Prescribed	✓	×	−14.9	−241.1	−116.3	−267.2	−320.7	−312.4	−276.5	−267.8
Prescribed	×	✓	139.6	−110.0	26.8	459.3	304.3	364.6	–	–
Sim./presc.	×	×	2.6	−224.2	−100.5	0.1	−49.7	−44.5	–	–

2.5. *Simulation protocol and spin-up*

In the standard setup, the BernCC model is forced with land cover data for cropland, pasture, and built-up area and emissions of CO_2 and of other radiative agents and precursor substances. Data-based emission estimates are used for the industrial period (Fuglestvedt and Berntsen, 1999; Joos et al., 2001) and projected emissions for the IIASA A2, B1 and B2 scenarios.

For the assessment of the impact of land use on the carbon cycle, on CO_2 and climate, simulations with land use are compared to corresponding baseline simulations without land use.

A range of sensitivity simulations were performed to quantify the importance of individual processes on the impact of land use on carbon fluxes and climate variables (Table 1 provides the results for scenario A2; corresponding results for scenarios B1, B2 are given in Table 7). Many previous studies using spatially explicit land use data considered only the evolution of cropland (e.g. McGuire et al., 2001; Brovkin et al., 2004), but not changes in pasture. Correspondingly, we ran 'no pasture' simulations considering only cropland and built-up area. Earlier studies (Joos et al., 2001; Gerber et al., 2004) identified the stimulation of carbon uptake by rising CO_2 levels enhancing water use efficiency (CO_2 fertilization) and the release of carbon in response to heat stress and accelerated soil respiration under warming climate as the dominant mechanisms governing changes in carbon storage in LPJ-DGVM. In the 'constant climate' simulations, the climate sensitivity is set to zero and no long-term climate change is simulated. In the 'no CO_2 fertilization' simulations, CO_2 is kept at its pre-industrial value in the LPJ-DGVM module.

Atmospheric CO_2 would have evolved differently in the absence of LULUC than observed. Different atmospheric CO_2 concentration histories yield different evolutions of climate (in response to CO_2 forcing) and of terrestrial carbon stocks (in response to CO_2 fertilization and climate change). Thus, to be able to estimate the total earth system impact of LULUC, we use a standard model setup where atmospheric CO_2 is simulated throughout the whole simulated period. Consequently, the baseline simulation and the simulation with land use have different CO_2 concentrations and climate.

In addition, simulations have been performed with atmospheric CO_2 before 2000 A.D. prescribed according to observations ('CO_2 prescribed'). The historical part of these simulations is compared with earlier studies using terrestrial models off-line (e.g. McGuire et al., 2001). The future part, on the other hand, is used to compare different scenarios of land use (with and without pasture) and emissions and land use change (A2, B1, B2) with a common starting point at the year 2000.

The inertia related to land use processes and the commitment of past LULUC on future atmospheric CO_2 and climate is quantified with simulations in which land use change is stalled at 2000.

LPJ-DGVM is spun up from bare ground for 1000 yr under pre-industrial CO_2, a baseline climate that includes interannual variability (Leemans and Cramer, 1991; Cramer et al., 2001) and the land cover distribution for 1700 AD. At year 400, soil carbon is set to the equilibrium value corresponding to current litter input and decomposition rates. The spin-up is continued for another 600 yr to reach equilibrium. No spin-up is required for the other BernCC model components. In transient simulations, the LPJ-DGVM module is forced by the boundary conditions as described in Sections 2.3 and 2.4.

2.6. *Land use flux analysis*

The impact of LULUC on the terrestrial carbon cycle is assessed as the difference L in the net terrestrial uptake F between the simulations without land use (nolu) and with land use (lu):

$$L = F_{\mathrm{nolu}} - F_{\mathrm{lu}}. \tag{4}$$

Note that the evolution of CO_2 and climate is different in the two cases, as described in the previous section. L includes carbon (release) fluxes caused by land use and (uptake) fluxes prevented by land use, and can be formally regarded as a net flux, here referred to as land use flux.

L can be split into three terms for each grid cell. The first represents the consequence of the removal of natural vegetation, and its replacement with agricultural vegetation on croplands/pastures (which are also exposed to different CO_2/climate under the land use scenario). As will be discussed in Section 3, the main effect of this replacement is a loss of carbon sinks, because natural forests accumulate more carbon under elevated CO_2 than do cropland and pasture. The second-term captures the effect that the change in atmospheric CO_2 and climate due to LULUC affects uptake on natural lands. Hence the name 'land use feedback'. The third term describes the release of carbon through harvest losses and decay of wood products from the conversion of natural land (see Fig. 2). In sum,

$$L = \underbrace{\Delta A(n_{\mathrm{nolu}} - u_{\mathrm{lu}})}_{\text{'replaced sinks/sources'}} + \underbrace{A_{\mathrm{lu}}\Delta n}_{\text{'land use feedback'}} + \underbrace{\int_{t0}^{t} \frac{\mathrm{d}A_{\mathrm{lu}}}{\mathrm{d}t'} r(t-t')t't_0 t}_{\text{harvest loss and products}}, \quad (5)$$

where A is the area of natural lands, n is the net carbon uptake (including disturbance) on natural land, u is the net uptake on used land, Δ denotes differences between simulations without land use and with land use. Thus, ΔA is the area under land use and Δn is the difference in net uptake on natural land between the simulation without and with land use. Note that A_{lu} is the *natural* area in the *land use* case. t is time and t_0 refers to the pre-industrial initial state of the simulation.

The fate of carbon on converted land simulated by the model as described in Section 2.3 is governed by the overturning time scales of products, soil and litter pools. It is symbolically represented in eq. (5) by a 'response function' r. How is our approach related to other approaches to quantify a land use carbon flux? Modelling studies with prescribed CO_2 concentrations (e.g. McGuire et al., 2001) neglect the effect of LULUC on CO_2 and climate. Consequently, the 'land use feedback' is also neglected, and the 'replaced sinks/sources' flux is computed with the net uptake flux on natural land (n) simulated for prescribed (observed) CO_2 instead of the hypothetical CO_2 concentration corresponding to a scenario without LULUC.

The book-keeping approach neglects any interactions between climate, CO_2 and terrestrial carbon fluxes, captured by the lost sinks and land use feedback terms, and includes only carbon emissions directly related to the conversion of natural land and regrowth on abandoned land.

Of the fluxes accounted for in a book-keeping model, the product decay term in LPJ covers the immediate carbon loss to the atmosphere during harvest and fluxes from the product pools. The remaining fluxes contribute to the 'replaced sinks/sources' term: Harvest losses that enter the land use litter pools affect the net uptake flux on area under land use (u) in LPJ. Similarly, regrowth is treated as part of the uptake on natural land (n) in LPJ.

The book-keeping approach corresponds approximately to calculating L from simulations without climate change and CO_2 fertilization.[1] The book-keeping flux is also roughly comparable to the sum of the changes in carbon stocks on the converted lands as given in Table 2 (differences arise because the table is derived from a simulation with prescribed historical CO_2 and climate affecting carbon fluxes, and does not include the product pools).

Our set of sensitivity simulations (Table 1) was also used to estimate the contributions of CO_2 fertilization and climate to the individual terms in eq. (5), as detailed in Appendix A (the individual fluxes are shown in Table 3 and Fig. 8).

The fluxes contributing to L that are considered in the book-keeping approach scale roughly with the rate of land conversion ($\mathrm{d}A/\mathrm{d}t$). These fluxes will vanish on the typical time scales of regrowth and decay of products and slash if the transformation of land is halted. In contrast, the fluxes related to feedbacks with atmospheric CO_2 and climate scale either with the area under land use ('replaced sinks/sources') or with the area covered by natural land ('land use feedback'). These fluxes will be of continuous importance even after land transformation is halted.

3. Results

3.1. Role of land use during the past 300 yr

As expected, the simulation without land use fails to reproduce the historical atmospheric CO_2 concentrations from ice core and atmospheric measurements (Fig. 3). The model performance is much improved by considering land use. Using the full land use data set including pasture gives a good match with the record over most of the industrial period. In the latter half of the 20th century, atmospheric CO_2 is overestimated by about 10 ppm. Here, the measurement data are bracketed by the simulations with and without pasture.

Land use is found to be an important contributor in the historical carbon budget, in agreement with earlier estimates (see Houghton, 2003 and references therein). Land use leads to a loss of 188 Gt C of terrestrial carbon by the year 2000 in the standard simulation. This is comparable to the cumulative fossil CO_2 emissions of 274 Gt. When the effect of pastures is neglected, the land use flux is 84 Gt C. Thus pasture and cropland have an impact of comparable magnitude, in contrast to other studies that rank pasture second in importance to cropland (e.g. Houghton and Goodale, 2004).

[1] The book-keeping fluxes presented here were calculated with the product decay flux taken from the standard simulation, which is not exactly the same as in the simulation without climate change and CO_2 fertilization.

Table 2. Breakdown by biomes of carbon stocks in 1700 (after spinup) and stock changes by 2000 for a simulation with prescribed atmospheric CO_2 including cropland, built-up area and pasture. Totals are subdivided into landuse categories in 2000 and carbon pools. Land use categories considered include areas in use (crop/built-up or pasture) since pre-industrial times ('old LU'), areas turned into cropland/built-up ('new cropland') and pasture by 2000 ('new pasture'), and remaining natural area in 2000 including abandoned land ('natural'). Carbon pools include live vegetation and the combined litter and soil pools. Biomes are determined from the simulated vegetation after spinup using the algorithm described in Joos et al. (2004). Temperate and warm temperate forest from Joos et al. (2004) are lumped together as 'temperate'; tropical desert, tundra and polar biomes are lumped together as 'other'. Summing initial carbon and carbon change over all land use categories gives total terrestrial carbon at 1700 and the difference in terrestrial carbon between 1700 and 2000, respectively. Carbon stock densities and changes per area can be obtained by dividing each value by the corresponding area given in rows 1–4

	Global	Tropical forest	Temperate forest	Boreal forest	Tundra-forest	Savannah	Dry grass/ shrub	Others
Areas in year 2000 (Mio. km^2)								
Old LU	6.9	0.5	1.7	0.3	0.0	1.9	1.9	0.7
New cropland	13.4	2.0	3.3	0.6	0.0	4.0	3.2	0.4
New pasture	29.7	3.3	2.2	0.9	0.1	7.4	11.5	4.3
Natural	81.9	15.2	8.1	15.8	2.7	9.7	12.3	18.0
Carbon stocks in year 1700 (Pg C)								
Vegetation								
Old LU	4.1	0.2	1.4	0.2	0.0	1.2	1.0	0.1
New cropland	85.3	25.5	32.6	5.6	0.0	17.5	4.0	0.1
New pasture	119.7	43.2	23.8	9.5	0.4	30.4	11.9	0.6
Natural	574.2	233.1	89.4	174.7	18.2	42.8	12.0	3.8
Soil and litter								
Old LU	76.0	2.0	26.0	8.7	0.1	23.6	14.3	1.4
New cropland	154.8	14.9	50.5	17.6	0.1	50.2	20.8	0.7
New pasture	258.1	25.6	31.9	29.6	1.0	96.5	63.5	10.2
Natural	1046.9	111.0	141.5	474.6	75.8	116.3	68.9	58.8
Change in carbon stocks from 1700 to 2000 (Pg C)								
Vegetation								
Old LU	0.5	0.0	0.3	0.0	0.0	0.1	0.0	0.0
New cropland	−76.8	−24.5	−29.7	−5.0	−0.0	−15.1	−2.4	−0.0
New pasture	−103.5	−41.1	−21.3	−8.8	−0.3	−25.5	−6.5	0.0
Natural	36.0	20.0	4.7	1.1	0.4	6.0	2.7	1.1
Soil and litter								
Old LU	5.9	0.5	1.3	0.4	−0.0	2.6	1.0	0.1
New cropland	−18.2	−5.3	−4.1	−0.9	0.0	−7.1	−0.8	0.1
New pasture	−8.7	−8.7	−0.2	−0.1	0.2	−7.7	6.2	1.6
Natural	35.1	8.7	2.9	6.7	1.0	4.5	5.3	6.1

The impact per unit area is higher for cropland than for pasture, since cropland accounts for only 30–40% of the land use area in the HYDE3.0 data set. The consequences of land conversion for carbon storage depends on the biome affected. A breakdown of converted areas, carbon stocks and stock changes by biome was calculated using the biome mapping scheme described in Joos et al. (2004) (Table 2). It shows that almost 80% of the area converted for pasture since 1700 is claimed from natural lands without closed forest cover (Table 2). The remaining 20%, however contribute about 70% of the direct carbon emissions, owing to much greater biomass density of forests (tropic, temperate and boreal; Table 2). Consequently, carbon emissions calculated from LUC are sensitive to errors in the simulated extent of natural forests.

To assess the possibility of overestimated carbon emissions due to conversion of forest to pasture, an attribution of converted areas to biomes similar to that in Table 2 was done for a simulation using the HYDE2.0 data set. Pasture areas converted from different biomes were also computed based on the biome distribution given in the HYDE2.0 data set (the HYDE3.0 data do not contain biome information and can therefore not be used for this comparison). In the simulation, 5.5 Mio. km^2 of forested lands, and 21.3 Mio. km^2 from non-forest lands are converted to pasture over the period from 1700 to 1990 spanned by the land use data. These values are similar to those shown in Table 2 for the standard simulation. The original HYDE2.0 data yield 8.7 Mio. km^2 pasture claimed from forested lands, and 21.9 Mio. km^2 from non-forest lands. The total natural areas converted to pasture do

Table 3. Land use flux and components in standard model setup, based on biospheric uptake results with simulated CO_2 (corresponding to Table 1, rows 1–3 and 7).

Cumulated flux (Gt C)	1700–1999	2000–2099 A2
Total	**188**	**211**
Cropland + built-up	84	112
Pasture	104	99
Book-keeping	**232**	**56**
Products + losses	247	64
Regrowth	−15	−8
Replaced sinks/sources	**11**	**115**
Fertilization	0	121
Climate	11	−6
LU Feedback	**−43**	**−3**
Fertilization	−57	7
Climate	13	−10
Nonlinear interactions	**−12**	**44**

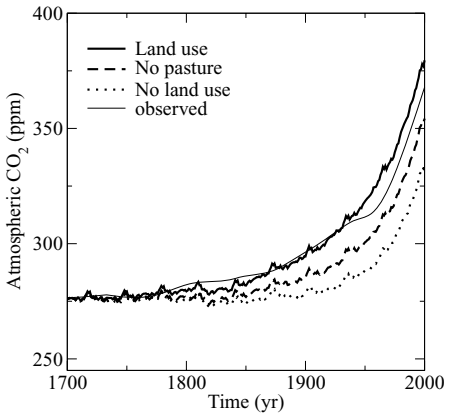

Fig. 3. Atmospheric CO_2 in simulations for 1700–2000 in comparison with a spline through ice core and atmospheric CO_2 data (Tom Conway, personal communication, 2006; Meure et al., 2006; Keeling and Whorf, 2003).

not agree, because conversions of pasture to cropland, which are common in the original data are partly masked by the aggregation on the coarser LPJ grid. Consequently, conversion of natural areas is attributed to cropland and pasture proportionally. Nevertheless, the magnitude of the simulated deforested area due to pasture expansion compares well with the HYDE2.0 data set, suggesting that this is not a major source of error. Also, the carbon losses on formerly forested and non-forested lands converted to pasture computed for the HYDE2.0 simulation (−73.2 and −40.1 Pg, respectively) are quite similar to the losses reported in Table 2 (−80.5 and −31.7 Pg).

Emissions also strongly depend on biomass densities. Biomass densities can be computed from Table 2 by dividing carbon stocks by the corresponding areas. Brovkin et al. (2004)

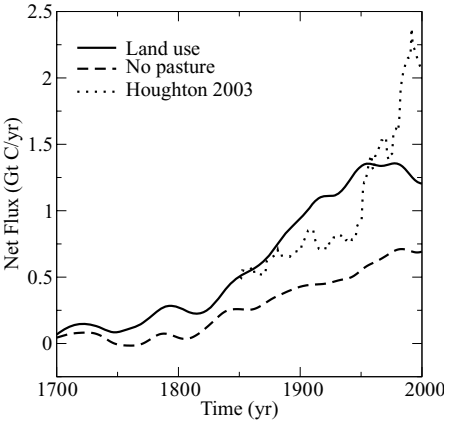

Fig. 4. Simulated land use fluxes in the past 300 yr with standard model setup. The land use fluxes calculated by Houghton (2003) are shown for comparison.

report that LPJ tends to overpredict carbon storage in the forests and woodlands of European Russia and Eastern Europe. A comparison with other publications suggests that the biomass densities simulated by our version of LPJ are also too high in temperate and boreal forests (Sabine et al., 2004b; Houghton, 2005), although Houghton (1999) reports similar values as simulated here.

Simulated global land use flux (Fig. 4) is below 0.3 Gt yr^{-1} until about 1825 and from then on increases almost linearly to about 1.7 Gt C yr^{-1} in 1950. Land use flux remains constant until 1980 and decreases slightly afterwards. When the impact of pastures is neglected, a near-linear increase results, from close to zero in 1800 and before to 0.75 Gt yr^{-1} in 2000. The land use flux estimate by Houghton (2003) for the time before 1950 lies between the results from the standard simulation and the one neglecting pastures (Fig. 4). The Houghton estimate for the second half of the 20th century shows a sharp increase, in contrast to our results. According to Houghton (2003), this reflects tropical deforestation in that period. Similar results as reported here were found by McGuire et al. (2001). Also, recent satellite-based studies find a tropical deforestation flux compatible with our results (Table 4; Achard et al. 2002, DeFries et al. 2002).

As DeFries et al. (2002) use a book-keeping model basically identical to that of Houghton (2003), much of the discrepancy between these two estimates can be ascribed to differences in the land use data used. Similar to DeFries et al. (2002), our simulations are based partly on satellite data, which may explain why the results are also similar. The contribution from wood harvest (without permanent clearing) and shifting cultivation may be a significant one that is not included in our model. Its true importance is, however, highly uncertain, owing to the poor data available about shifting cultivation (e.g. Houghton and Goodale, 2004). On the other hand, our estimate (like McGuire et al., 2001) takes into account the influence of CO_2 and climate.

Table 4. Land use flux estimates for the eighties and nineties

Land use flux (Gt C yr^{-1})	Tropics		Global	
	1980s	1990s	1980s	1990s
This study	1.26	1.02	1.54	1.08
Houghton (2003)	1.93 ± 0.6	2.2 ± 0.6	1.99 ± 0.8	2.18 ± 0.8
McGuire et al. (2001)	0.5–1.2	–	0.6–1.0	–
DeFries et al. (2002)	0.65	0.97	–	–
Achard et al. (2002)	–	0.96	–	–

These factors affect the land use flux significantly, as discussed in Section 3.6.

3.2. Pre-industrial LULUC impact estimate

A considerable area had been used as croplands and pastures already in 1700. According to the HYDE3.0 data, land use was concentrated in Europe, central and east Asia at the time, and comprised about 5% of the global land area. Although not explicitly simulated, the impact of this pre-industrial LULUC in terms of a land use flux can be roughly estimated by comparing the initial states of the simulations with and without land use. This implies the assumptions that LULUC occurred slowly enough for the terrestrial carbon pools to be near steady state, and that carbon stored in wood products is negligible. After the spinup, the terrestrial biosphere in the simulation without LULUC stores about 2360 Gt carbon, 45 Gt more than in the land use simulation (23 more than in the simulation without pasture), which may be regarded as an estimate of the integrated pre-industrial land use flux. If released to the atmosphere at once, this would have caused the atmospheric CO_2 concentration to increase by 21 ppm (11 ppm without pasture), using a conversion factor of 2.121 Gt C ppm^{-1}. However, in the course of the centuries to millennia over which these emissions occurred, most of the carbon added to the atmosphere will have been absorbed by the ocean, allowing for a CO_2 rise of merely a few ppm (with an airborne fraction of about 14% for a 1000 yr of ocean uptake, the effect is about 3 ppm, or 1.5 ppm when neglecting pastures). This pre-industrial anthropogenic effect can thus account for at best a small fraction of the observed rise of about 25 ppm over the Holocene or an anthropogenic contribution of 14 ppm as postulated by Ruddiman (2005). The same applies to the impact on climate (with 3 ppm corresponding to less than 0.05 °C global equilibrium temperature change for an equilibrium climate sensitivity of 3 °C).

3.3. How large is the terrestrial sink?

The record of historical atmospheric CO_2 from direct measurements and ice core data provides a boundary condition useful for constraining the exchange fluxes between the components of the global carbon cycle, for example, Siegenthaler and Oeschger (1987), Enting et al. (1995) and Joos et al. (1999). The simulated net terrestrial uptake fluxes are compared with independent estimates from atmospheric oxygen and CO_2 observations (Plattner et al., 2002; Manning and Keeling, 2006) and with results of a (updated) single deconvolution of the atmospheric CO_2 record (Joos et al., 1999) (Fig. 5). In the single deconvolution, the net change in terrestrial carbon storage is computed as the difference between fossil emissions (Marland et al., 2006) and the

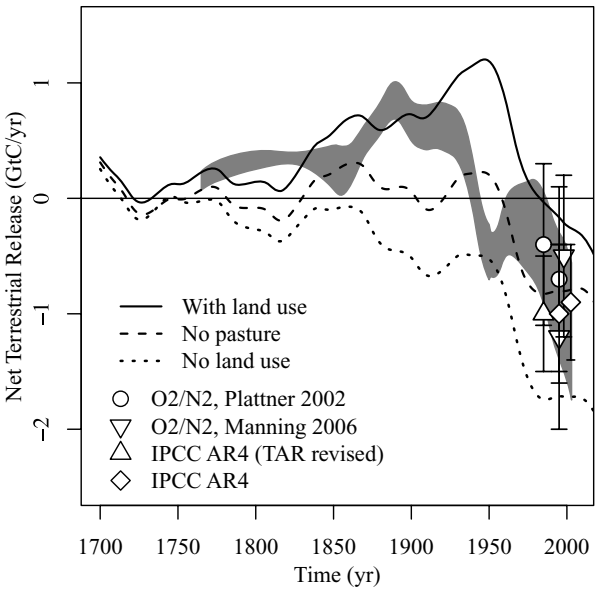

Fig. 5. Net carbon flux from the terrestrial biosphere to the atmosphere. Lines: simulations with standard model setup and different land use maps (a smoothing spline with a 55 yr cutoff period was applied). Symbols: Independent estimates (Manning and Keeling, 2006; Plattner et al., 2002) with corresponding standard errors (bars; horizontal whiskers mark the time period of each estimate). Shaded band: flux inferred from budgeting fossil emissions, ocean uptake and atmospheric CO_2, including an error range of ± 1 std. dev. due to uncertainties in atmospheric CO_2 as estimated by Joos et al. (1999), and due to uncertainties in ocean uptake, taken as 20% and industrial emissions, taken as 10% before 1950, and 5% after 1950 (Bruno and Joos, 1997).

Table 5. Carbon budget for historical simulations with LULUC using the prescribed CO_2 record (Table 1, row 4) to infer the terrestrial carbon exchange flux. Numbers in brackets refer to the simulation without pasture. The error estimates refer to ± 1 *SD*. and correspond to the shaded band in Fig. 5; errors due to uncertainties in atmospheric CO_2 (Joos et al., 1999) are treated as independent from year to year; relative ocean uptake (20%) and industrial emission uncertainties (10% before 1950, and 5% after 1950; Bruno and Joos, 1997) are assumed to be constant over the respective integration periods.

C exchange (Gt C)	1700–1999	1980–1989	1990–1999
Atmospheric increase[a]	193 ± 2	32 ± 0	33 ± 0
Industrial emissions[b]	274 ± 17	54 ± 3	64 ± 3
Ocean-atmosphere flux	-156 ± 31	-21 ± 4	-23 ± 5
Land-atmosphere flux from budget	75 ± 36	-2 ± 5	-7 ± 6
Simulated land-atmosphere flux	123 (−13)	−2 (−11)	−1 (−6)
Flux unexplained by simulation	−48 (89)	−1 (8)	−6 (−1)
Land use flux[c]	188 (84)	15 (9)	11 (6)
Residual terrestrial sink	−113 (−8)	−18 (−11)	−18 (−13)

[a]Meure et al. (2006), Keeling and Whorf (2003), Tom Conway pers. comm.
[b]Marland et al. (2006).
[c]Estimate based on run with simulated CO_2 (Table 1, row 1).

change in observed atmospheric and simulated oceanic carbon inventories. The simulated ocean carbon uptake of 137 Gt C between 1800 and 1994 is somewhat larger than the estimate of 118 ± 19 Gt C during the same period by Sabine et al. (2004a). On the other hand, the ocean uptake of 23 Gt C for the 1990s, simulated with prescribed CO_2, compares very well with the most recent estimate by the Intergovernmental Panel on Climate Change (Denman et al., 2007) of 22 ± 4 Gt C. Results from the LULUC simulation compare reasonably well with these independent estimates. In contrast, the simulation without land use does not match up with these estimates, in accordance with the comparison of atmospheric CO_2 pressure with the measurement record (Fig. 3).

The cumulative budget-derived net fluxes are summarized in Table 5 for the simulated period from 1700 to 2000, and for the eighties and nineties, along with the global net land-to-atmosphere carbon fluxes as simulated by LPJ under the prescribed historical CO_2 levels and LULUC scenarios. The simulated terrestrial carbon release over the entire historical period is about 50 Gt C larger than the central estimate from the single deconvolution. This difference is just within the uncertainty of the single deconvolution estimate ($2\,SD = 72$ Gt C). On the other hand, the simulated release in the land use simulations without pasture is almost 90 Gt C smaller than the single deconvolution estimate. Although the difference between simulated and budget-derived terrestrial release might be explained by uncertainties in the single deconvolution approach, there are likely additional factors contributing: (i) errors in the representation of LULUC given by model (omitted known processes) and data limitations; (ii) unquantified error due to parameter uncertainties in the model and (iii) additional processes not known or accounted for.

In the last two decades before 2000, results from single deconvolution and LULUC simulation agree within $\pm$ one SD. It is tempting to attribute this to an improving quality of LULUC data towards the present. However, the detailed history of the fluxes (Fig. 5) does not support this interpretation, because most of the disagreement between the budget and the simulated uptake arises in the two decades around 1950, while before and after this period, the two estimates are compatible (Fig. 5). This roughly corresponds to the time when the simulated CO_2 concentration (with full LULUC) is seen to depart from the observations, which show a temporary break in the steady rising CO_2 trend (Fig. 3). The latter is not completely understood, but may be caused by ENSO-related decadal climate variability affecting the ocean and perhaps terrestrial uptake of CO_2, a process not represented in the model (Etheridge et al., 1996). Overprediction of land use emissions is an alternative possible reason for the overestimated CO_2 concentrations in this period, for example, due to too high simulated biomass combined with intense land use change (see also Section 3.1; Brovkin et al., 2004).

A comparison of the land-atmosphere flux inferred from single deconvolution with the land use flux estimate suggests that there has been a significant terrestrial carbon sink in the past, known as the 'residual sink' (Denman et al., 2007). Our results suggest that the residual sink flux was on average 1.8 Gt C yr^{-1} over the 1980s and 1990s and amounted to 113 Gt C over the period 1700 to 1999 AD (Table 5). LPJ provides a plausible sink mechanism by CO_2 fertilization, which is however still too weak in the standard

model setup to allow the model to closely reproduce the observed atmospheric CO_2 concentrations.

3.4. Land use in the 21st century

By the year 2100, atmospheric CO_2 concentrations are projected to rise to about 990, 590 and 710 ppm in A2, B1 and B2, respectively, with the standard model setup (Fig. 6). The corresponding increases in global mean temperature over pre-industrial levels are 4.2, 2.8 and 3.2 K, respectively (Fig. 6). Only in the scenario B1 the global change is seen to decelerate, while both A2 and B2 show a steadily rising trend in CO_2 and temperature until 2100.

Net terrestrial carbon uptake differs strongly between the scenarios A2, B1 and B2, and even more between the simulations with and without LULUC (Fig. 6). In its consequences for atmospheric CO_2 and climate, these differences in terrestrial carbon uptake are dwarfed by the inter-scenario differences in industrial emissions. By 2100, LULUC results at most (i.e. in A2) in an additional 72 ppm CO_2 or 0.18 K warming, respectively. In comparison, scenarios A2 and B1 differ by 395 ppm or 1.37 K in 2100 (with land use included).

These results are sensitive to the uncertainty in the strength of CO_2 fertilization and climate change (Fig. 7). Between the simulations where either fertilization or climate change is shut off, the spread in atmospheric CO_2 by the year 2100 is 270 ppm for scenario A2. The temperature range, including only the fertilization sensitivity, is 0.33 K (the simulation with climate sensitivity set to zero shows the impact of climate on CO_2 but not the feedback on the global temperature).

Fertilization acts as a negative feedback by absorbing some of the anthropogenic CO_2. Climate provides a positive feedback on uptake similar in size and opposed to the fertilization feedback. With LULUC taken into account, the net terrestrial uptake over this century is only about 60 Gt C for A2 with standard settings.

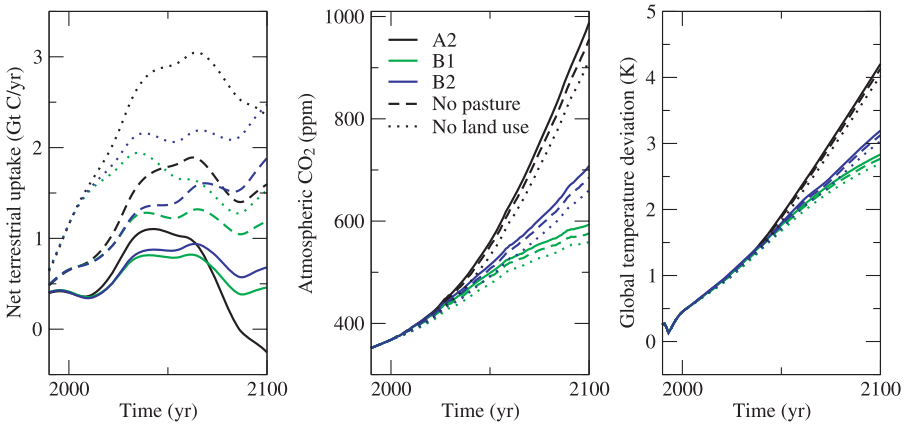

Fig. 6. Net terrestrial carbon uptake, atmospheric CO_2, and global temperature deviation for different fossil emission and land use scenarios. Before 2000, CO_2 is prescribed and net uptake is inferred from the CO_2 budget. The net uptake curves are not perfectly aligned in 2000 because of the spline smoothing applied.

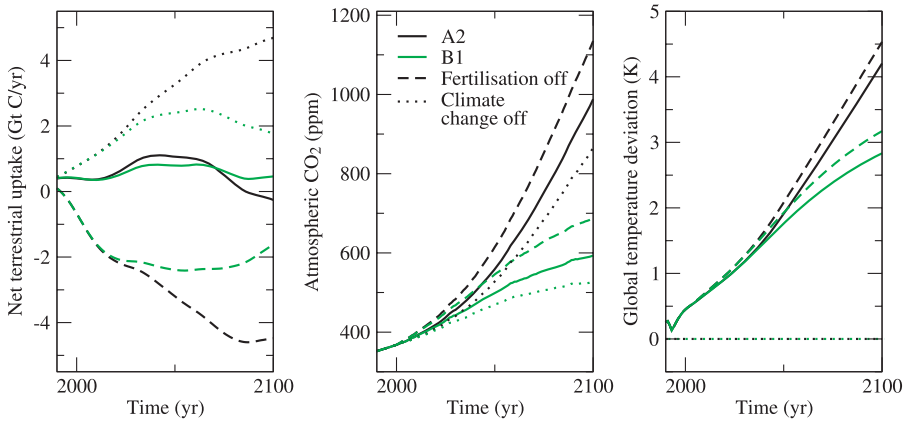

Fig. 7. Net terrestrial carbon uptake, atmospheric CO_2, and global temperature deviation for scenarios A2 and B1 with sensitivity settings and full land use. Before 2000, CO_2 is prescribed and net uptake is inferred from the CO_2 budget. The net uptake curves are not perfectly aligned in 2000 because of the spline smoothing applied.

Table 6. Projected land use flux in the 21st century (in Gt C yr^{-1}), based on biospheric uptake results with simulated CO_2 (corresponding to Table 1, rows 1–3 and 7)

Model setup	A2	B1	B2
LU flux, standard	211	103	145
LU flux, fertilization off	51	35	44
Book-keeping flux	56	32	–
Feedback+lost sinks+interactions	155	72	–
Commitment from past LULUC	150	80	104

In contrast, setting the climate sensitivity to zero results in an uptake of about 300 Gt C in A2, whereas shutting off fertilization results in a release of almost 400 Gt C.

Interestingly, while terrestrial uptake is higher in A2 when there is no climate change, it is higher in B2 when there is no fertilization. Also, when climate change is excluded, the negative fertilization feedback decreases the scenario-dependent spread in atmospheric CO_2, while when climate alone is considered, the spread is increased due to the positive climate feedback.

Our estimates of the global land use flux in the 21st century of about 100–200 Gt C (Tables 6 and 3, Fig. 8) is comparable to the historical flux in absolute terms. As noted, its relative contribution to the carbon budget decreases in relation to growing industrial emissions. The model uncertainty illustrated by the sensitivity simulations is reflected in the land use flux, particularly the uncertainty related to CO_2 fertilization (Table 6). The mechanisms of this interaction are investigated in Section 3.6.

3.5. Effect of global change on terrestrial carbon uptake

In LPJ, terrestrial carbon storage (Fig. 9) reacts to rising atmospheric CO_2 pressure and climate change in a number of ways: CO_2 fertilization enhances the uptake of carbon globally, and drives the biosphere towards a higher equilibrium carbon stock. The total uptake per unit area is globally quite uniform, except for somewhat higher uptake in the tropics and lower uptake in northern Siberia (cf. Table 2). In the tropics, it is the vegetation that stores most of the carbon added. In the temperate and boreal zones, soils take up an amount comparable to vegetation, because the slow decay of soil carbon allows for significant carbon storage.

Climate change leads to an increase in carbon at the northern fringe of boreal forests, which can be attributed to a northward migration of the treeline. In the temperate and boreal areas, carbon is released for two reasons: first, higher decay rates of soil carbon due to higher temperatures, and second, a reduction in forest areas in favour of grasslands. The latter is related partly to a strong reduction in the abundance of the boreal needle-leaved PFT due to heat stress, partly to a change in soil water availability. Thus, while loss of carbon dominates in simulations considering climate alone, in combination with fertilization a pattern of a northward-shift in carbon storage is seen in the northern hemisphere. In the tropics, the effect of climate change is a minor decrease of carbon stored in soils. Apart from that, climate change also interacts with fertilization to enhance or decrease uptake. Except for forest dieback, these changes are already seen in the historical simulations, particularly in the high latitudes, where climate signals are amplified. In the future part of the scenario simulations, the drivers and consequently, the effects, are much stronger.

3.6. Mechanisms of land use impact on the terrestrial carbon cycle

Land use interacts with this changing terrestrial biosphere as described by eq. (5) in Section 2.6. Using this equation, the different components contributing to the land use flux were quantified (Table 3). The most obvious and direct land use impact

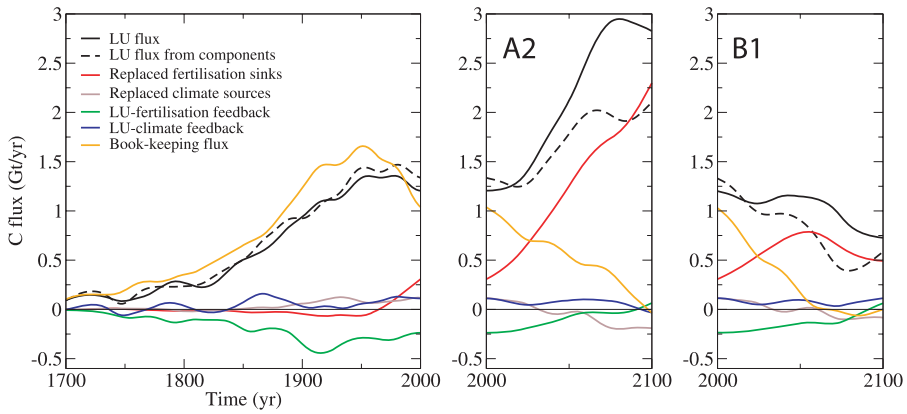

Fig. 8. Land use flux and estimated component fluxes for the past and for scenarios A2 and B1. The sum of land use components (black dashed) falls short of the total land use flux (black solid) due to nonlinear interactions between carbon fluxes, CO_2 and climate not included in the individual components. The component fluxes are explained in Section 3.6, definitions are given in Appendix A.

Table 7. Net biospheric uptake in Gt C for scenarios B1, B2 and corresponding commitment runs. Dashes indicate settings for which no simulation was performed.

Historical CO_2	Climate change	CO_2 fertil.	B1, 21st century			B2, 21st century			B1 commitment		B2 commitment	
			No LU	LU	LU, no pasture	No LU	LU	LU, no pasture	LU	LU, no pasture	LU	LU, no pasture
Simulated	✓	✓	161.1	57.6	115.0	206.2	61.2	136.4	81.2	135.5	101.8	172.8
Simulated	✓	×	−186.8	−221.5	−211.9	−204.4	−248.5	−244.3	–	–	–	–
Simulated	×	✓	273.6	198.1	233.9	–	–	–	–	–	–	–
Simulated	×	×	0.1	−28.6	−23.9	0.1	−39.1	−34.2	–	–	–	–
Prescribed	✓	✓	162.4	58.4	109.4	202.6	67.1	129.6	80.9	130.5	105.9	167.2
Prescribed	✓	×	−178.9	−214.4	−206.1	−197.5	−243.4	−234.0	−192.2	−183.4	−210.4	−199.9
Prescribed	×	✓	276.9	198.3	–	–	–	–	–	–	–	–
Prescribed	×	×	0.1	−28.6	–	–	–	–	–	–	–	–

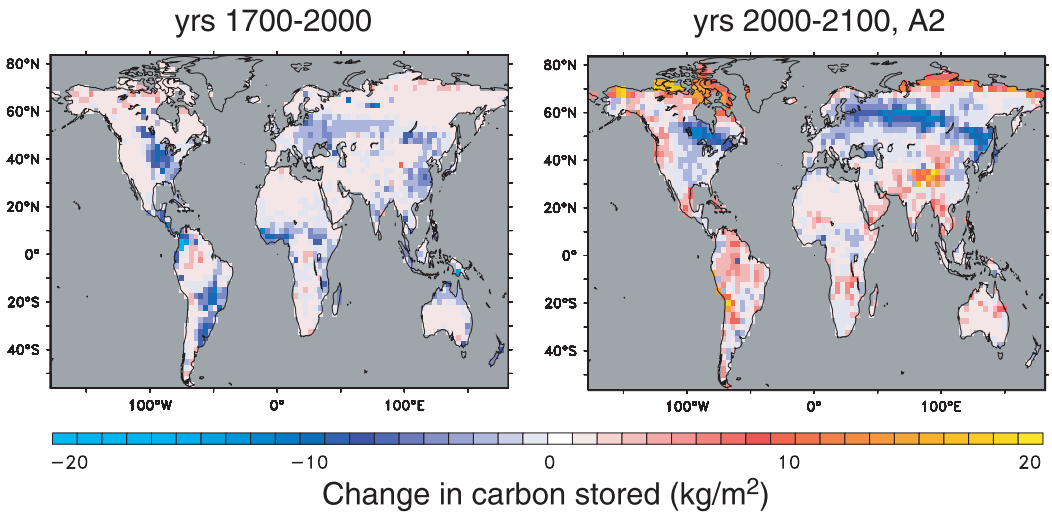

Fig. 9. Change in terrestrial carbon storage in the past (1700–2000) and for the future (2000–2100, scenario A2) with standard model setup, considering cropland, pasture, and built-up area.

corresponds to the book-keeping flux, including the term 'product flux and harvest loss' and release of carbon from litter and soils following deforestation (included in the term 'replaced sinks/sources'). The book-keeping flux makes up the bulk of the LULUC flux in the past (Fig. 8). Spatially, it corresponds neatly to the pattern of historical land use change (Fig. 10).

In comparison to the book-keeping study of Houghton (2003), our book-keeping flux is higher at all times up to the mid-20th century, and the mismatch during that period is greater than with our total land use flux. The disagreement in the latter half of the 20th century, on the other hand, remains much the same.

The land use flux is modified by CO_2 fertilization. Fertilization provides a negative feedback in that land use CO_2 emissions stimulate CO_2 uptake. This land use fertilization feedback, which reduces the impact of land use on atmospheric CO_2 and climate is important in the past, amounting to about 25% of the book-keeping flux [land use feedback in eq. (5), Fig. 8]. As indicated by eq. (5), the fertilization feedback is effective globally and correlates with the extent of forests (Fig. 10).

A corresponding feedback effect exists with regard to climate change (eq. 5 and Appendix A). The land use-climate feedback enhances both the treeline extension in the north and the carbon loss further south. Because these processes are opposed, a minor net flux results (Fig. 8). The remaining processes ('replaced sinks/sources', CO_2-climate interactions) give rise to only small fluxes in the past because of the overall as yet moderate CO_2/climate change.

For the future scenarios, the situation is largely reversed: Because land use as a driver becomes secondary to fossil emissions, so do the book-keeping and the fertilization feedback processes, which are driven by land use itself. Instead, it is now the interactions of land use with exogenously raised CO_2 levels that make up the bulk of the land use impact. The leading process is the replacement of forests, acting as a CO_2-enhanced sink, by

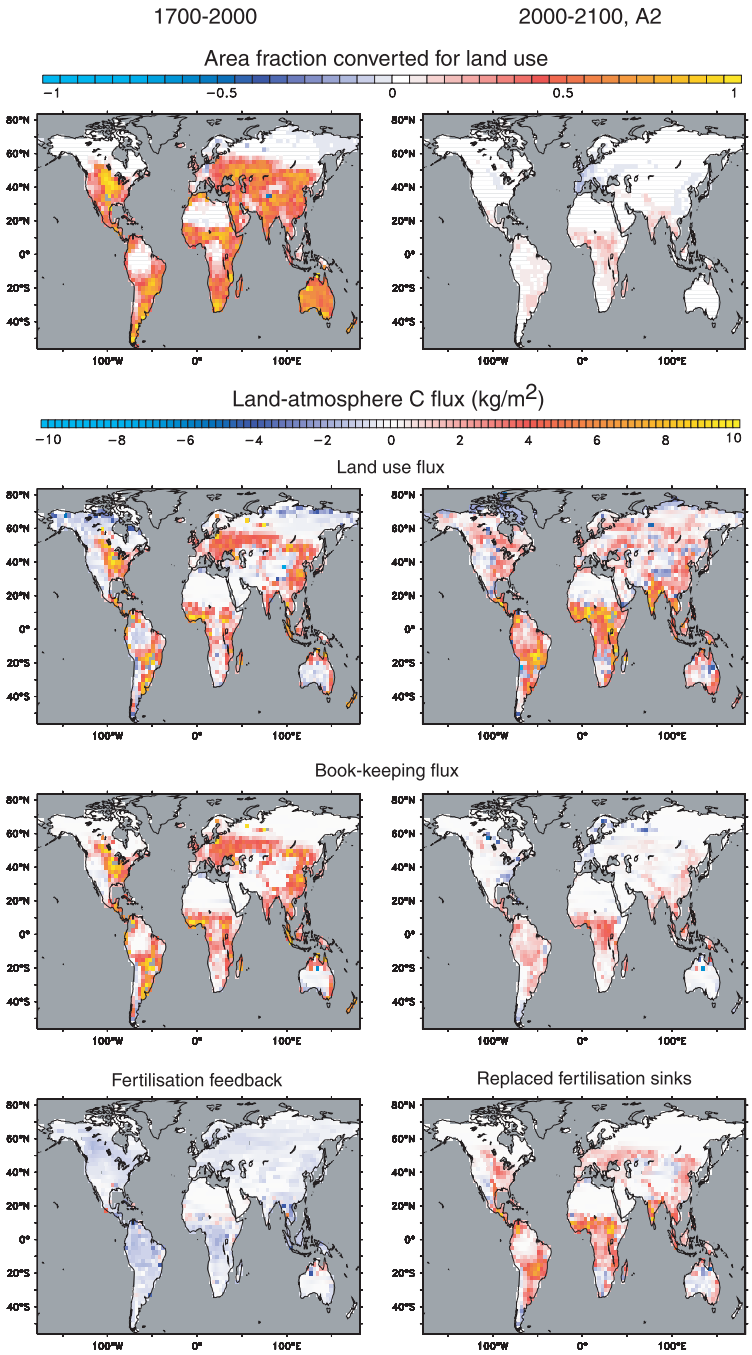

Fig. 10. Spatial distribution of land use area change (top row) and land use fluxes (rows 2–4) for standard model setup and future scenario A2. Integrated over historical time (left-hand column) and 21 century (right-hand colum), respectively.

non-forest areas, which are weaker sinks (Fig. 8), resulting in a net lost sink. Gitz and Ciais (2003, 2004) have called this the land-use amplifier effect.

Thus, the difference in net terrestrial carbon uptake between scenarios is driven in the first place by the vastly different fossil emission rather than the land use scenarios themselves. The interaction with climate change further amplifies the impact of lost natural fertilization sinks or vice versa (represented by the difference between the actual and additive land use fluxes in Fig. 8). In accordance with the treatment laid out in Section 2.6, these 'replaced sinks/sources' fluxes correlate spatially with the total land use area ΔA (Fig. 10). This said, the scenarios used here project the use of arable land associated with simulated future food production, and hence do not consider a possible more extreme deforestation. Stronger deforestation could also be caused by further expansion of pasture area, which is kept

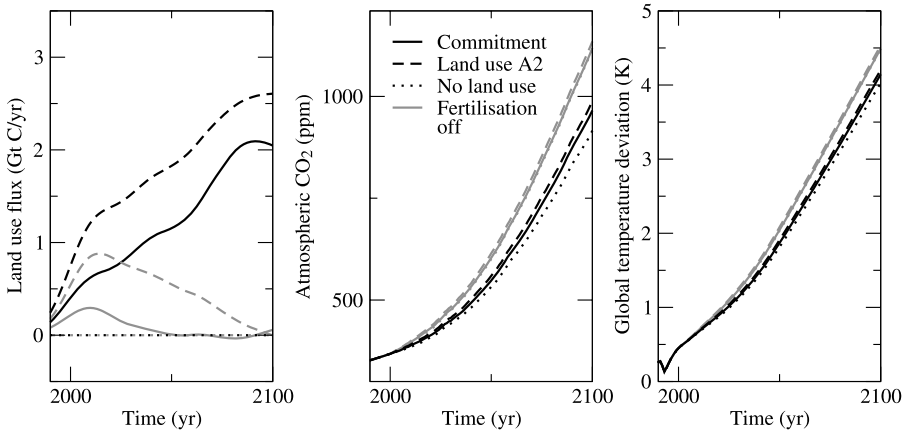

Fig. 11. Land use commitment: land use flux, atmospheric CO_2, and global mean temperature deviation simulated with the standard model setup for scenario A2, for a commitment run with land use area kept constant after 2000, and for a run without land use (black). Similar simulations with CO_2 fertilization shut off are shown in grey.

approximately constant after 2000 due to the lack of a future scenario for pastures.

3.7. Land use commitment

The lost fertilization sinks, which have a potential to dominate the future land use impact, are related to the total land use area, not to ongoing land use change. In the scenarios used here, most of this area is already cleared by 2000, and human appropriation of land is indeed more limited than fossil emissions in that it cannot surpass historical levels by orders of magnitude. Thus, historical and current land use plays a potentially big role in the carbon cycle in the future. We quantify this role using the concept of 'land use commitment', which we define as the land use flux in a simulation in which land use area is kept constant after 2000, while fossil emissions evolve according to the scenarios (Fig. 11).

A comparison of the land use commitment over the 21st century with the scenario land use fluxes (Table 6) shows that much of the future land use impact can be considered as already committed. Thus land use represents a legacy of human interaction with atmospheric CO_2 and ultimately, climate.

4. Discussion and conclusions

The role of LULUC in the carbon cycle with its implications for climate in the past and the future was investigated. The BernCC model, which includes the Lund–Potsdam–Jena dynamic global vegetation model (Gerber et al., 2003) was complemented with a spatially explicit representation of croplands, pastures, and built-up areas and their evolution over time. Estimates of land use area in the past were combined with post-SRES scenarios (A2, B1 and B2) into continuous land use scenarios from 1700 to 2100.

While the scenarios used here roughly span the range of industrial emissions given by the SRES/TAR illustrative marker scenarios, they all depict relatively small land use changes in the 21st century. Total land use area remains close to the present extent in all these scenarios. The overall importance of LULUC in the 21st century is overshadowed by the growing fossil CO_2 emissions in the scenarios considered. This is likely to be the case even in much more extreme deforestation scenarios.

LULUC leads to higher atmospheric CO_2 by causing release and preventing uptake of CO_2 by the terrestrial biosphere. This land use flux results from qualitatively different processes: (i) the 'book-keeping flux' includes C fluxes that result directly from land use change, as simulated by book-keeping models; (ii) the 'replaced sinks/sources' describe a net carbon loss on converted lands due to the replacement of natural vegetation by agriculture, which is less efficient as a carbon sink in LPJ and (iii) the 'land-use feedback' accounts for the effect of LULUC-induced changes in atmospheric CO_2 and climate on the productivity of the remaining natural lands.

The book-keeping flux has been dominating over the industrial period until the present. Its share in anthropogenic CO_2 emissions is comparable in magnitude to the cumulative fossil emissions. Accordingly, the land use flux must be accounted for in any model to realistically simulate atmospheric CO_2 and climate over the industrial period. This is successfully done in our land use model, which is based on spatially explicit representation of land use areas as an integrated part of the terrestrial biosphere. This approach is preferable over an exogenously prescribed deforestation flux, because the feedback between LULUC and atmospheric CO_2 and climate are accounted for. The land use-fertilization feedback has been important in the past. Although secondary to the book-keeping flux, the simulated fertilization feedback has led to a reduction of the net land use flux by about 25% of the book-keeping flux.

In the future scenarios, the 'replaced sinks/sources' flux increases in parallel with rising atmospheric CO_2. It surpasses the book-keeping and land-use feedback fluxes. Lost sinks are

essentially the areas under land use. In the scenarios used here, most of the area under land use by 2100 is already converted today. Consequently, there is a commitment to future climate change due to past LULUC. Possible scenarios featuring more extreme deforestation scenarios would imply higher book-keeping fluxes. However, as more deforestation would also mean more natural carbon sinks lost and higher CO_2, the commitment flux is likely to remain dominant in a large range of conceivable scenarios. Thus the conclusion is robust in that respect that most of the future LULUC land use flux is due to a commitment from past land use change.

The importance of the land use commitment leads us to de-emphasize the traditional book-keeping flux when considering the role of LULUC in the future. This conclusion hinges on the magnitude of productivity stimulation by elevated CO_2, and other factors not explicitly considered here, such as nitrogen deposition. A similar commitment effect could arise from different soil overturning rates on agricultural versus natural land. The effectiveness of these mechanisms and of CO_2 fertilization in particular in real ecosystems and under much higher CO_2 levels is still very unclear. Therefore, to understand the role of LULUC, we need to understand fertilization mechanisms.

The global carbon budget suggests a strong residual sink, which is commonly attributed to the terrestrial biosphere. In the model, CO_2 fertilization provides such a terrestrial sink, which is required to realistically reproduce historic CO_2 concentrations. This sink is indeed still too weak to match the residual sink inferred from the global carbon budget. On the other hand, this mismatch could equally well be due to the omission or misrepresentation of another process, whether related to land use or not. Our land use model omits forestry as well as other management practices, which are partly accounted for in Houghton (2003). However, Houghton and Goodale (2004) argues that these are of secondary importance in comparison to cropland and pasture expansion. The role of shifting cultivation and forest degradation is potentially more important (Houghton and Goodale, 2004), but is hardly quantifiable for lack of reliable data. In light of this uncertainty, we see the 'first-order approach' of including only the reasonably quantifiable and important effects justified.

In contrast to most previous studies, the newly available HYDE3.0 data allowed us to take pastures into account, at least for the past and to some extent into the future. Although the land use flux per unit area from pastures is on average smaller than that of cropland, due to the larger spatial extent of pastures, both cropland and pasture are of similar importance. In contrast, Houghton and Goodale (2004) rank LULUC for pasture secondary in importance to cropland with a carbon source a third the size of the latter. Apart from the latter half of 20th century, our book-keeping flux estimates are higher than those by Houghton (2003), which also include pasture. Part of this discrepancy most likely stems from the input data; a discussion of their limitations is beyond the scope of this paper. But a significant remaining difference may be due to the way land conversion for pasture is modelled.

Deviations between simulated and actual vegetation distribution are one source of error. However, the distribution of pasture areas claimed from forested vs. non-forested biomes in a simulation using the HYDE2.0 data is similar to that obtained from the biome distribution given in the original HYDE2.0 data set. This result does not suggest major errors to arise from the simulated vegetation distribution. Another possibility is that pasture expansion does not affect the natural vegetation as strongly as assumed here. Houghton (1999), e.g., assumes that pastures are claimed from natural grassland in North America and China, without affecting carbon storage. For comparison, we estimate losses in total carbon due to pasture expansion on savannah and dry grass/shrub lands of 34 Gt C worldwide (Table 2). A third possibility is overprediction of biomass per area. Brovkin et al. (2004) relate overprediction of CO_2 emissions to cropland changes in the 1950s in temperate regions with too high simulated carbon stocks. A similar effect might contribute to the overestimate of CO_2 seen here (Fig. 3), although in the HYDE3.0 data the timing and spatial distribution of LUC does not show such a clear pattern as in the data of Ramankutty and Foley (1999) used by Brovkin et al. (2004). Data on carbon stocks of different biomes have large uncertainties (Houghton, 1999; Sabine et al., 2004b; Houghton, 2005). The recent assessment by Sabine et al. (2004b) suggests that LPJ strongly overpredicts carbon storage in boreal forests, and underpredicts soil carbon storage in tropical forests. Boreal forests only contribute about 15 Gt C to the total simulated emissions of about 200 Gt C (Table 2). Emissions from tropical soils might be some 20 Gt higher than the estimated 14 Gt found here (Table 2). In conclusion, the global land use flux is not strongly biased by any one of these sources of error.

This study does not account for biogeophysical effects of LULUC, as described by Sitch et al. (2005), Brovkin et al. (2004). The leading biogeophysical effect of LULUC arises from the strong difference in albedo between snow-covered forests and grassland. Although there is considerable uncertainty in the quantification of this albedo difference in state-of-the-art climate models (Roesch, 2006), it should be noted that the LULUC-related albedo change results in a cooling effect opposed to and potentially compensating or even overcompensating the radiative forcing of the land use CO_2 flux (Bala et al., 2007).

Ruddiman (2005) presents an update of his 'anthropogenic hypothesis', according to which land use caused the atmospheric CO_2 increase of about 14 ppm over the past 11 kyr. This anthropogenic CO_2 rise is supposed to have prevented a cooling of the global climate and the onset of a new ice age. Based on the HYDE land use map for 1700 we estimate the potential impact of LULUC on atmospheric CO_2 in pre-industrial times to a few ppm—much less than the postulated 14 ppm. Accordingly, the potential impact of pre-industrial anthropogenic emissions on climate is negligibly small.

5. Acknowledgments

This work was funded by the International Institute of Applied System Analysis, Vienna, in the framework of the Global Greenhouse Initiative and the Gains-Asia programs. We would like to thank the scientists from IIASA who have contributed to this work with helpful comments and discussions. We are also indebted to Gian-Kasper Plattner, whose suggestions and critical remarks helped improve this manuscript. Special thanks are due to Kees Klein Goldewijk for providing the HYDE3.0 data set as well as helpful and encouraging comments to the study.

6. Appendix A: Land use components

The deviation of the net terrestrial uptake from initial equilibrium can be separated approximately into the effects of CO_2, climate, and a remainder including in our model harvest losses and regrowth terms (fluctuations are neglected).

$$n = n_{CO_2} + n_{\mathrm{Clim}} + n_{\mathrm{regrowth}} \tag{A1}$$

$$u = u_{CO_2} + u_{\mathrm{Clim}} + u_{\text{harvest loss}}, \tag{A2}$$

where n and u are the net terrestrial uptake on natural and used lands, respectively. These terms are quantified using sensitivity simulations where climate sensitivity is zero (s0), or alternatively, fertilization is shut off (f0). The biospheric uptake terms appearing in eq. (5) are estimated as

$$n_{\mathrm{nolu}} \simeq \underbrace{\left(n^{s0}_{\mathrm{nolu}} - n^{s0,f0}_{\mathrm{nolu}}\right)}_{CO_2} + \underbrace{\left(n^{f0}_{\mathrm{nolu}} - n^{s0,f0}_{\mathrm{nolu}}\right)}_{\mathrm{Clim}} + \underbrace{n^{s0,f0}_{\mathrm{nolu}}}_{\simeq 0} \tag{A3}$$

$$u_{\mathrm{lu}} \simeq \underbrace{\left(u^{s0}_{\mathrm{lu}} - u^{s0,f0}_{\mathrm{lu}}\right)}_{CO_2} + \underbrace{\left(u^{f0}_{\mathrm{lu}} - u^{s0,f0}_{\mathrm{lu}}\right)}_{\mathrm{Clim}} + \underbrace{u^{s0,f0}_{\mathrm{lu}}}_{\text{harvest loss}} \tag{A4}$$

$$\begin{aligned}\Delta n \simeq\ & \underbrace{\left(n^{s0}_{\mathrm{nolu}} - n^{s0,f0}_{\mathrm{nolu}}\right) - \left(n^{s0}_{\mathrm{lu}} - n^{s0,f0}_{\mathrm{lu}}\right)}_{CO_2} \\ & + \underbrace{\left(n^{f0}_{\mathrm{nolu}} - n^{s0,f0}_{\mathrm{nolu}}\right) - \left(n^{f0}_{\mathrm{lu}} - n^{s0,f0}_{\mathrm{lu}}\right)}_{\mathrm{Clim}} \\ & + \underbrace{n^{s0,f0}_{\mathrm{nolu}} - n^{s0,f0}_{\mathrm{lu}}}_{\mathrm{regrowth}}.\end{aligned} \tag{A5}$$

Expanding eq. (5) to use these approximations yields

$$\begin{aligned}L =\ & \text{i. Replaced fertilization sinks} \\ & \text{ii. Replaced climate sinks/sources} \\ & \text{iii. Land use-fertilization feedback} \\ & \text{iv. Land use-climate feedback} \\ & \text{v. Book-keeping flux} \\ & \text{vi. Interaction terms}\end{aligned} \tag{A6}$$

$$\begin{aligned}=\ & \text{i. } \Delta A\left(\left(n^{s0}_{\mathrm{nolu}} - n^{s0f0}_{\mathrm{nolu}}\right) - \left(u^{s0}_{\mathrm{lu}} - u^{s0f0}_{\mathrm{lu}}\right)\right) + \\ & \text{ii. } \Delta A\left(\left(n^{f0}_{\mathrm{nolu}} - n^{s0f0}_{\mathrm{nolu}}\right) - \left(u^{f0}_{\mathrm{lu}} - u^{s0f0}_{\mathrm{lu}}\right)\right) + \\ & \text{iii. } A_{\mathrm{lu}}\left(\left(n^{s0}_{\mathrm{nolu}} - n^{s0f0}_{\mathrm{nolu}}\right) - \left(n^{s0}_{\mathrm{lu}} - n^{s0f0}_{\mathrm{lu}}\right)\right) + \\ & \text{iv. } A_{\mathrm{lu}}\left(\left(n^{f0}_{\mathrm{nolu}} - n^{s0f0}_{\mathrm{nolu}}\right) - \left(n^{f0}_{\mathrm{lu}} - n^{s0f0}_{\mathrm{lu}}\right)\right) + \\ & \text{v. } \Delta A\left(n^{s0f0}_{\mathrm{nolu}} - u^{s0f0}_{\mathrm{lu}}\right) + A_{\mathrm{lu}}\left(n^{s0f0}_{\mathrm{nolu}} - n^{s0f0}_{\mathrm{lu}}\right) + P \\ & \text{vi. } \begin{cases} +\Delta A\left[\left(n_{\mathrm{nolu}} + n^{s0f0}_{\mathrm{nolu}}\right) - \left(n^{s0}_{\mathrm{nolu}} + n^{f0}_{\mathrm{nolu}}\right)\right. \\ \left. -\left(u_{\mathrm{lu}} + u^{s0f0}_{\mathrm{lu}}\right) + \left(u^{s0}_{\mathrm{lu}} + u^{f0}_{\mathrm{lu}}\right)\right] \\ +A_{\mathrm{lu}}\left[\left(n_{\mathrm{nolu}} - n_{\mathrm{lu}}\right) + \left(n^{s0f0}_{\mathrm{nolu}} - n^{s0f0}_{\mathrm{lu}}\right)\right. \\ \left. -\left(n^{s0}_{\mathrm{nolu}} - n^{s0}_{\mathrm{lu}}\right) - \left(n^{f0}_{\mathrm{nolu}} - n^{f0}_{\mathrm{lu}}\right)\right], \end{cases}\end{aligned} \tag{A7}$$

where P is the product decay flux, n is net uptake in the actual simulation, L is the land use flux derived from the standard simulations including all effects, the sum of terms i-v is the land use flux assuming additive effects of CO_2 and climate, and term vi represents the interaction between the two. In the calculations presented, built-up area is accounted for separately. It constitutes a minor contribution and is neglected here for simplicity.

7. Appendix B: Light competition scheme

In LPJ, competition for light is based on the fractional plant cover (FPC) of each plant functional type (PFT), and the constraint that the sum of FPCs cannot exceed unity. This means that the maximum cross section on which light is absorbed is equal to the surface area of the grid cell. Increase of FPC in excess of this limit is corrected for by shading mortality. The distribution of shading mortality among the PFTs present in a given grid cell determines how light competition works.

In the Sitch et al. (2003) version of LPJ, shading mortality 'is partitioned among woody PFTs in proportion to the FPC increment resulting from their biomass increment for this year.' This biomass increase is determined by the subroutine calculating NPP. If this were the only process affecting FPC, this algorithm would exactly cancel the growth of each PFT in excess of the available area. Consequently, in a cell in which FPC is at its maximal value in a given year, any change to distribution of FPC per PFT would be cancelled, so that the cell would maintain its current distribution indefinitely, unless any of the PFTs are affected by other processes like growing conditions turning worse due to climate change. In effect, competition would be limited to the primary establishment of vegetation from bare ground.

However, in LPJ, FPC is also changed when new plant individuals are established, due to the added biomass of saplings. Establishment typically happens on a yearly basis. This has two implications. First, as the correction applied to each PFT does not exactly correspond to that PFTs status, the number of plants of the given PFT to be removed can at times exceed the number present. This must be corrected for to avoid negative plant densities. Second, competition is strongly enhanced. In particular, the

tropical broad-leaved evergreen PFT gets a strong competitive advantage, allowing it under certain circumstances to displace all other PFTs.

For the present study, the partitioning of shading mortality was changed: shading is partitioned in proportion to the total FPC of each PFT, as opposed to the FPC increment. This approach avoids the aforementioned problems while allowing for reasonable competition among PFTs.

References

Achard, F., Eva, H. D., Stibig, H. J., Mayaux, P., Gallego, J. and co-authors. 2002. Determination of deforestation rates of the world's humid tropical forests. *Science* **297**, 999–1002.

Bala, G., Caldeira, K., Wickett, M., Phillips, T. J., Lobell, D. B. and co-authors. 2007. Combined climate and carbon-cycle effects of large-scale deforestation. *Proc. Natl. Acad. Sci. USA* **104**, 6550–6555, doi:10.1073/pnas.0608998104.

Bondeau, A., Smith, P. C., Zaehle, S., Schaphoff, S., Lucht, W. and co-authors. 2007. Modelling the role of agriculture for the 20th century global terrestrial carbon balance. *Global Change Biol.* **13**, 1–28, doi:10.1111/j.1365-2486.2006.01305.x.

Brovkin, V., Sitch, S., von Bloh, W., Claussen, M., Bauer, E. and co-authors. 2004. Role of land cover changes for atmospheric CO_2 increase and climate change during the last 150 years. *Global Change Biol.* **10**, 1253–1266.

Brovkin, V., Claussen, M., Driesschaert, E., Fichefet, T., Kicklighter, D. and co-authors. 2006. Biogeophysical effects of historical land cover changes simulated by six earth system models of intermediate complexity. *Clim. Dyn.* **26**, 587–600, doi:10.1007/s00382-005-0092-6.

Bruno, M. and Joos, F. 1997. Terrestrial carbon storage during the past 200 years: a Monte Carlo analysis of CO_2 data from ice core and atmospheric measurements. *Global Biogeochem. Cycles* **11**(1), 111–124.

Cramer, W., Bondeau, A., Woodward, F. I., Prentice, I. C., Betts, R. A. and co-authors. 2001. Global response of terrestrial ecosystem structure and function to CO_2 and climate change: results from six global dynamic vegetation models. *Global Change Biol.* **7**, 357–373.

Cubasch, U. R., Voss, R., Hegerl, G. C., Waszkewitz, J. and Crowley, T. J. 1997. Simulation of the influence of solar radiation variations on the global climate with an ocean-atmosphere general circulation model. *Clim. Dyn.* **13**, 757–767.

DeFries, R. S., Houghton, R. A., Hansen, M. C., Field, C. B., Skole, D. and co-authors. 2002. Carbon emissions from tropical deforestation and regrowth based on satellite observations for the 1980s and 1990s. *Proc. Natl. Acad. Sci. USA* **99**, 14256–14261.

Denman, K. L., Brasseur, G., Chidthaisong, A., Ciais, P., Cox, P. and co-authors. 2007. Couplings between changes in the climate system and biogeochemistry. In: *Climate Change 2007: The Physical Science Basis. Contribution of Working Group I to the Fourth Assessment Report of the Intergovernmental Panel on Climate Change*, Chapter 7 (ed. S. Solomon), Cambridge Univ. Press, New York.

Edmonds, J., Joos, F., Nakićenović, N., Richels, R. G. and Sarmiento, J. L. 2004. Scenarios, targets, gaps, and costs. In: *The Global Carbon Cycle: Integrating humans, climate, and the natural world* (eds C. B. Field and M. R. Raupach), Island Press, Washington, SCOPE 62, chap. Scenarios, Targets, Gaps, and Costs.

Enting, I. G., Trudinger, C. M. and Francey, R. J. 1995. A synthesis inversion of the concentration and $\delta^{13}C$ of atmospheric CO_2. *Tellus* **47B**, 35–52.

Etheridge, D. M., Steele, L. P., Langenfelds, R. L., Francey, R. J., Barnola, J. M. and co-authors. 1996. Natural and anthropogenic changes in atmospheric CO_2 over the last 1000 years from air in Antarctic ice and firn. *J. Geophys. Res.* **101**, 4115–4128.

Farquhar, G. D., von Caemmerer, S. and Berry, J. A. 1980. A biochemical model of photosynthetic CO_2 assimilation in leaves of C_3 species. *Planta* **149**, 78–90.

Feddema, J. J., Oleson, K. W., Bonan, G. B., Mearns, L. O., Buja, L. E. and co-authors. 2005. The importance of land-cover change in simulating future climates. *Science* **310**, 1674–1678.

Field, C. B. and Raupach, M. R. (eds.), 2004. *The Global Carbon Cycle: Integrating Humans, Climate, and the Natural World*. SCOPE 62. Island Press, Washington.

Foley, J. A. 1995. An equilibrium model of the terrestrial carbon budget. *Tellus* **47B**, 310–319.

Forster, P., Ramaswamy, V., Artaxo, P., Berntsen, T., Betts, R. A. and co-authors. 2007. Changes in atmospheric constituents and in radiative forcing. In: *Climate Change 2007: The Physical Science Basis. Contribution of Working Group I to the Fourth Assessment Report of the Intergovernmental Panel on Climate Change*, Chapter 2 (ed. S. Solomon), Cambridge Univ. Press, New York.

Fuglestvedt, J. and Berntsen, T. 1999. A simple model for scenario studies of changes in global climate. Working Paper 1999:2, Center for International Climate and Environmental Research, Oslo. ISSN:0804-452x.

Gerber, S., Joos, F., Brügger, P., Stocker, T. F., Mann, M. E. and co-authors. 2003. Constraining temperature variations over the last millennium by comparing simulated and observed atmospheric CO_2. *Clim. Dyn.* **20**, 281–299, doi:10.1007/s00382-002-0270-8.

Gerber, S., Joos, F. and Prentice, I. C. 2004. Sensitvity of a dynamic global vegetation model to climate and atmospheric CO_2. *Global Change Biol.* **10**, 1223–1239.

Gitz, V. and Ciais, P. 2003. Amplification effect of changes in land use and concentration of atmospheric CO_2. *Comptes Rendus Geosci.* **335**, 1179–1198.

Gitz, V. and Ciais, P. 2004. Future expansion of agriculture and pasture acts to amplify atmospheric CO_2 levels in response to fossil-fuel and land-use change emissions. *Clim. Change* **67**, 161–184.

Goodale, C. L., Apps, M. J., Birdsey, R. A., Field, C. B., Heath, L. S. and co-authors. 2002. Forest carbon sinks in the northern hemisphere. *Ecol. Appl.* **12**, 891–899.

Haxeltine, A. and Prentice, I. C. 1996. BIOME 3: an equilibrium terrestrial biosphere model based on ecophysiological constraints, resource availability and competition among plant functional types. *Global Biogeochem. Cycles* **10**, 693–703.

Houghton, R. A. 1999. The annual net flux of carbon to the atmosphere from changes in land use 1850–1990. *Tellus* **51B**, 298–313.

Houghton, R. A. 2003. Revised estimates of the annual net flux of carbon to the atmosphere from changes in land use and land management 1850–2000. *Tellus* **55B**, 378–390.

Houghton, R. A., Hobbie, J. E., Melillo, J. M., Moore, B., Peterson, B. J. and co-authors. 1983. Changes in the carbon content of terrestrial

biota and soils between 1860 and 1980—a net release of CO_2 to the atmosphere. *Ecol. Monogr.* **53**, 235–262.

Houghton, R. A., Joos, F. and Asner, G. P. 2004. The effects of land use and managment on the global carbon cycle. In: *Land Change Science: Observing, Monitoring, and Understanding Trajectories of Change on the Earth's Surface* (ed. G. Gutman), Springer, Remote Sensing and Digital Image Processing, Vol. 6, E-book., ISBN: 1-4020-2562–9.

Houghton, R. and Goodale, C. 2004. Effects of land-use change on the carbon balance of terrestrial ecosystems. In: *Ecosystems and Land Use Change* (eds R. DeFries, G. Asner and R. Houghton), American Geophysical Union, Washington, DC.

Houghton, R. A. 2005. Aboveground forest biomass and the global carbon balance. *Global Change Biol.* **11**, 945–958.

Hurtt, G. C., Pacala, S. W., Moorcroft, P. R., Caspersen, J., Shevliakova, E. and co-authors. 2002. Projecting the future of the U. S. carbon sink. *Proc. Natl. Acad. Sci. USA* **99**, 1389–1394, doi:10.1073/pnas.012249999.

Joos, F., Bruno, M., Fink, R., Stocker, T. F., Siegenthaler, U. and co-authors. 1996. An efficient and accurate representation of complex oceanic and biospheric models of anthropogenic carbon uptake. *Tellus* **48B**, 397–417.

Joos, F., Meyer, R., Bruno, M. and Leuenberger, M. 1999. The variability in the carbon sinks as reconstructed for the last 1000 years. *Geophys. Res. Lett.* **26**, 1437–1441.

Joos, F., Prentice, I. C., Sitch, S., Meyer, R., Hooss, G. and co-authors. 2001. Global warming feedbacks on terrestrial carbon uptake under the Intergovernmental Panel on Climate Change (IPCC) emission scenarios. *Global Biogeochem. Cycles* **15**, 891–907.

Joos, F., Gerber, S., Prentice, I. C., Otto-Bliesner, B. L. and Valdes, P. J. 2004. Transient simulations of Holocene atmospheric carbon dioxide and terrestrial carbon since the Last Glacial Maximum. *Global Biogeochem. Cycles* **18**, 1–18. doi:10.

Keeling, C. D. and Whorf, T. P. 2003. Atmospheric CO_2 records from sites in the SIO air sampling network In: *Trends: A Compendium of Data on Global Change*, Carbon Dioxide Information Analysis Center,Oak Ridge National Laboratory, U.S. Department of Energy, Oak Ridge, Tenn., USA.

Klein Goldewijk, K. 2001. Estimating global land use change over the past 300 years: the HYDE database. *Global Biogeochem. Cycles* **15**, 417–433.

Klein Goldewijk, K. 2005. Three centuries of global population growth: a spatial referenced population (density) database for 1700–2000. *Populat. Environ.* **26**, 343–367.

Klein Goldewijk, K. and van Drecht, G. 2006. HYDE3: current and historical population and land cover. In: *Integrated modelling of global environmental change. An overview of IMAGE 2.4*. (eds A. F. Bouwman, T. Kram and K. Klein Goldewijk), Netherlands Environmental Assessment Agency (MNP), Bilthoven, The Netherlands.

Köhler, P., Joos, F., Gerber, S. and Knutti, R. 2005. Simulated changes in vegetation distribution, land carbon storage, and atmospheric CO_2 in response to a collapse of the North Atlantic thermohaline circulation. *Clim. Dyn.* **25**, 689–708.

Leemans, R. and Cramer, W. P. 1991. The IIASA climate database for land areas on a grid with 0.5° resolution. research report RR-91-18. Tech. rep., International Institute for Applied System Analysis.

Leemans, R., Eickhout, B., Strengers, B., Bouwman, L. and Schaeffer, M. 2002. The consequences for the terrestrial carbon cycle of uncertainties in land use, climate and vegetation responses in the IPCC SRES scenarios. *Sci. China* **45**, 126–141.

Lloyd, J. and Taylor, J. A. 1994. On the temperature dependence of soil respiration. *Funct. Ecol.* **8**, 315–323.

Manning, A. C. and Keeling, R. F. 2006. Global oceanic and land biotic carbon sinks from the Scripps atmospheric oxygen flask sampling network. *Tellus* **58B**, 95–116.

Marland, G., Boden, T. A. and Andres, R. J. 2006. Global, regional, and national CO_2 emissions. In: *Trends: A Compendium of Data on Global Change*, Carbon Dioxide Information Analysis Center, Oak Ridge National Laboratory, U.S. Department of Energy, Oak Ridge, Tenn., USA.

McGuire, A. D., Sitch, S., Clein, J. S., Dargaville, R., Esser, G. and co-authors. 2001. Carbon balance of the terrestrial biosphere in the twentieth century: analyses of CO_2, climate and land use effects with four process-based ecosystem models. *Global Biogeochem. Cycles* **15**, 183–206.

Meehl, G. A., Stocker, T. F., Collins, W. D., Friedlingstein, P., Gaye, A. T. and co-authors. 2007. Global climate projections. In: *Climate Change 2007: The Physical Science Basis. Contribution of Working Group I to the Fourth Assessment Report of the Intergovernmental Panel on Climate Change*, Chapter 10 (ed. S. Solomon), Cambridge Univ. Press, New York.

Messner, S. and Schrattenholzer, L. 2000. MESSAGE-MACRO: linking an energy supply model with a macroeconomic module and solving it iteratively. *Energy Int. J.* **25**, 267–282.

Meure, C. M., Etheridge, D., Trudinger, C., Steele, P., Langenfelds, R. and co-authors. 2006. Law dome CO_2, CH_4 and N_2O ice core records extended to 2000 years bp. *Geophys. Res. Lett.* **33**.

Mikolajewicz, U., Gröger, M., Maier-Reimer, R., Schurgers, G., Vizcaíno, M. and co-authors. 2007. Long-term effects of anthropogenic CO_2 emissions simulated with a complex earth system model. *Clim. Dyn.* **28**, 599–631, doi:10.1007/s00382-006-0204-y.

Monteith, J. L. 1995. Accommodation between transpiring vegetation and the convective boundary-layer. *J. Hydrol.* **166**, 251–263.

Mueller, C. and Lucht, W. 2007. Robustness of terrestrial carbon and water cycle simulations against variations in spatial resolution. *J. Geophys. Res.* **112D**, 1–7.

Nabuurs, G. J., Schelhaas, M. J., Mohren, G. M.J. and Field, C. B. 2003. Temporal evolution of the european forest sector carbon sink from 1950 to 1999. *Global Change Biol.* **9**, 152–160.

Nakićenović, N. and Swart, R. (eds.), 2000. *Special Report on Emission Scenarios*. Intergovernmental Panel on Climate Change, Cambridge University Press, New York.

Pacala, S. W., Hurtt, G. C., Baker, D., Peylin, P., Houghton, R. A. and co-authors. 2001. Consistent land- and atmosphere-based U.S. carbon sink estimates. *Science* **292**, 2316–2320.

Plattner, G. K., Joos, F. and Stocker, T. F. 2002. Revision of the global carbon budget due to changing air-sea oxygen fluxes. *Global Biogeochem. Cycles* **16**, 1096, doi:10.1029/2001GB001746.

Prather, M., Ehhalt, D., Dentener, F., Derwent, R., Dlugokencky, E. and co-authors. 2001. Atmospheric chemistry and greenhouse gases. In: *Climate Change 2001: The Scientific Basis. Contribution of Working Group I to the Third Assessment Report of the Intergovernmental Panel on Climate Change* (eds J. T. Houghton, Y. Ding, D. J. Griggs, M. Noguer, P. J. van der Linden, X. Dai, K. Maskell and C. A. Johnson), Cambridge Univ. Press, New York, 239–287.

Prentice, I. C., Farquhar, G. D., Fasham, M. J., Goulden, M. I., Heimann, M. and co-authors. 2001. The carbon cycle and atmospheric CO_2. In: *Climate Change 2001: The Scientific Basis. Contribution of Working Group I to the Third Assessment Report of the Intergovernmental Panel on Climate Change* (eds J. T. Houghton, Y. Ding, D. Griggs, M. Noguer, P. van der Linden, X. Dai, K. Maskell and C. A. Johnson), Cambridge University Press, Cambridge, United Kingdom and New York, NY, USA, 183–237.

Ramankutty, N. and Foley, J. A. 1999. Estimating historical changes in global land cover: croplands from 1700 to 1992. *Global Biogeochem. Cycles* **13**, 997–1027.

Riahi, K., Grubler, A. and Nakićenović, N. 2007. Scenarios of long-term socio-economic and environmental development under climate stabilization. *Technol. Forecast. Soc. Change* **74**, 887–935, doi:10.1016/j.techfore.2006.05.026.

Roesch, A. 2006. Evaluation of surface albedo and snow cover in AR4 coupled climate models. *J. Geophys. Res.* **111D**, 1–18.

Rokityanskiy, D., Benitez, P. C., Kraxner, F., McCallum, I., Obersteiner, M. and co-authors. 2006. Geographically explicit global modeling of land-use change, carbon sequestration, and biomass supply. *Technol. Forecast. Soc. Change* **74**, 1057–1082.

Ruddiman, W. F. 2005. Cold climate during the closest stage 11 analog to recent millennia. *Quarter. Sci. Rev.* **24**, 1111–1121.

Sabine, C. L., Feely, R. A., Gruber, N., Key, R. M., Lee, K. and co-authors. 2004a. The oceanic sink for anthropogenic CO_2. *Science* **305**, 367–371.

Sabine, C. L., Heimann, M., Artaxo, P., Bakker, D. C. E., Chen, C. T. A. and co-authors. 2004b. Current status and past trends of the global carbon cycle. In: *The Global Carbon Cycle: Integrating Humans, Climate and the Natural World* (eds C. B. Field and M. R. Raupach), Island Press, Washington, DC, 17–44.

Schimel, D., Alves, D., Enting, I. G., Heimann, M., Joos, F. and co-authors. 1996. CO_2 and the carbon cycle. In: *IPCC Second Scientific Assessment of Climate Change* (ed. J. T. Houghton), Cambridge Univ. Press, New York, 76–86.

Seneviratne, S. I., Lanthi, D., Litschi, M. and Schaer, C. 2006. Land-atmosphere coupling and climate change in europe. *Nature* **443**, 205–209.

Siegenthaler, U. and Joos, F. 1992. Use of a simple model for studying oceanic tracer distributions and the global carbon cycle. *Tellus* **44B**, 186–207.

Siegenthaler, U. and Oeschger, H. 1987. Biospheric CO_2 emissions during the past 200 years reconstructed by deconvolution of ice core data. *Tellus* **Ser. B, 39**, 140–154.

Sitch, S., Smith, B., Prentice, I. C., Arneth, A., Bondeau, A. and co-authors. 2003. Evaluation of ecosystem dynamics, plant geography and terrestrial carbon cycling in the LPJ dynamic global vegetation model. *Global Change Biol.* **9**, 161–185.

Sitch, S., Brovkin, V., von Bloh, W., van Vuuren, D., Eickhout, B. and Ganopolski, A. 2005. Impacts of future land cover changes on atmospheric CO_2 and climate. *Global Biogeochem. Cycles* **19**.

Strengers, B., Leemans, R., Eickhout, B., de Vries, B. and Bouwman, L. 2004. The land-use projections and resulting emissions in the IPCC SRES scenarios scenarios as simulated by the IMAGE 2.2 model. *GeoJournal* **61**, 381–393, doi:10.1007/s10708-004-5054-8.

Tubiello, F. N. and Fischer, G. 2006. Reducing climate change impacts on agriculture: global and regional effects of mitigation, 2000-2080. *Technol. Forecast. Soc. Change* **74**, 1030–1056, doi:10.1016/j.techfore.2006.05.027.

Vesala, T., Suni, T., Rannik, U., Keronen, P., Markkanen, T. and co-authors. 2005. Effect of thinning on surface fluxes in a boreal forest. *Global Biogeochem. Cycles* **19**.

Zobler, L. 1986. *A world soil file for global climate modelling*. Technical Memorandum 87802, NASA.